Optimal Location and Sizing of Dynamic VArs

for Fast Voltage Collapse

by

Ahmed Salloum

A Thesis Presented in Partial Fulfillment
of the Requirements for the Degree
Master of Science

Approved April 2011 by the
Graduate Supervisory Committee:

Vijay Vittal, Chair
Gerald Heydt
Raja Ayyanar

ARIZONA STATE UNIVERSITY

May 2011

ABSTRACT

Recent changes in the energy markets structure combined with the continuous load growth have caused power systems to be operated under more stressed conditions. In addition, the nature of power systems has also grown more complex and dynamic because of the increasing use of long inter-area tie-lines and the high motor loads especially those comprised mainly of residential single phase A/C motors. Therefore, delayed voltage recovery, fast voltage collapse and short term voltage stability issues in general have obtained significant importance in reliability studies. Shunt VAr injection has been used as a countermeasure for voltage instability. However, the dynamic and fast nature of short term voltage instability requires fast and sufficient VAr injection, and therefore dynamic VAr devices such as Static VAr Compensators (SVCs) and STATic COMpensators (STATCOMs) are used. The location and size of such devices are optimized in order to improve their efficiency and reduce initial costs. In this work time domain dynamic analysis was used to evaluate trajectory voltage sensitivities for each time step. Linear programming was then performed to determine the optimal amount of required VAr injection at each bus, using voltage sensitivities as weighting factors. Optimal VAr injection values from different operating conditions were weighted and averaged in order to obtain a final setting of the VAr requirement. Some buses under consideration were either assigned very small VAr injection values, or not assigned any value at all. Therefore, the approach used in this work was found to be useful in not only determining the optimal size of SVCs, but also their location.

TABLE OF CONTENTS

Page

CHAPTER Page

LIST OF TABLES

LIST OF FIGURES

Figure Page

LIST OF SYMBOLS

a_{pf}	Real power frequency sensitivity
a_{qf}	Reactive power frequency sensitivity
B	Net output susceptance
B_{im}	Imaginary part of the admittance matrix
B_{max}	Upper bound of susceptance
B_{min}	Lower bound of susceptance
FACTS	Flexible alternating current transmission system
$f(Qj)$	The value of the objective function at a given time instant
G_{im}	Real part of the admittance matrix
HVDC	High voltage direct current
I_i^*	The conjugate current injected at bus i.
I_m	Current drawn by motor
J	Jacobian matrix
J_r	Reduced Jacobian matrix
K	SVC gain
LMTF	Load modeling task force
LTC	Load tap changer transformer
MIDO	Mixed integer dynamic optimization
OPF	Optimal power flow
P	Real power

P_0	Real power consumed at rated voltage
P_1	Portion of real power modeled as constant impedance
P_2	Portion of real power modeled as constant current
P_3	Portion of real power modeled as constant power
P_i	Real power consumed at bus i
PMU	Phase measurement unit
PSLF	Positive sequence load flow
Q	Reactive power
Q_0	Reactive power consumed at rated voltage
Q_1	Portion of reactive power modeled as constant impedance
Q_2	Portion of reactive power modeled as constant current
Q_3	Portion of reactive power modeled as constant power
Q_i	Reactive power consumed at bus i
Q_j	Reactive power consumed at bus j
Q_{max}	Upper bound of injected reactive power
Q_{min}	Lower bound of injected reactive power
Q_T	The total weighted and averaged set of VAr

	injection values
R_r	Induction motor rotor resistance
R_s	Induction motor stator resistance
s	Slip
S_i	Apparent power consumed at bus i
STATCOM	Static compensator
SVC	Static VAr compensator
TSI_j	Trajectory sensitivity index for bus j
V_0	Rated bus voltage
VAr	Volt ampere reactive
$\|V_i\|$	Voltage magnitude at bus i
$\left\|V_i^0(t)\right\|$	Uncompensated voltage magnitude at bus i for a given time instant
V_m	Voltage magnitude at motor terminals
V_{max}	Maximum allowed voltage level
V_{min}	Minimum allowed voltage level
W_{bi}	Weighting factor for bus i
WECC	Western Electricity Coordinating Council
W_k	Weighting factor for time instant k
x	System state variable
X_m	Induction motor magnetizing reactance
X_r	Induction motor rotor reactance
X_s	Induction motor stator reactance

Y	Admittance matrix
ZIP	Composite static load model
Δf	Frequency mismatch
θ_i	Voltage phase angle at bus i

CHAPTER 1

INTRODUCTION

1.1 Overview

Recent voltage recovery delay events, or even fast voltage collapse incidents following a large disturbance, have resulted in voltage stability concerns acquiring an increased importance as a reliability issue [1]. For decades, angle stability problems had been given predominant attention in power system stability studies since it was considered to be responsible for most instability phenomena including voltage related events [2]. However, major changes in both, the structure of the power system and the way it is operated, have caused the voltage instability issue to be an independent phenomenon that can be initiated exclusively. Operating the system under stressed conditions, long inter-area tie lines, new -low inertia- generation sources and high motor loads, are all factors that have adversely affected the voltage response following a large disturbance especially near large load centers. The dynamic behavior of motor loads, such as decelerating and stalling, is considered the major cause of voltage recovery delay and fast voltage collapse incident especially in summer peaking load areas where low inertia single phase A/C motors comprise a significant portion of the load. However, in order to simplify the voltage stability issue and approach it more technically, it should be realized that reactive power deficiency is the basis of voltage instabilities no matter what the apparent reasons are.

Therefore, shunt reactive power injection has been used not only to increase the power transfer capabilities, but also as a voltage instability counter-

measure by providing reactive power support for the areas with reduced voltage profiles. However, the growing complexity of load behavior especially the fast highly nonlinear dynamic response of motor loads has imposed stringent requirements for reactive power compensation devices to be effective. Reactive power injection devices should have the capability of supporting short term voltage stability as well by preventing voltage recovery delay and voltage collapse events caused by fast acting dynamic loads. Therefore, Flexible AC Transmission System (FACTS) controllers are found to be more capable of providing dynamic reactive power compensation rather than fixed shunt capacitors. However, FACTS controllers should be located and sized carefully to obtain the desired reactive power support optimally.

1.2 Literature Review

Choosing the optimal location and size of reactive power injection devices has been considered a challenging multi-objective optimization problem [3]. This problem has been approached with a range of methodologies of various complexity levels. In [4], the objective is to determine the optimal size and location of shunt reactive power compensation devices. It is also desired to determine the right mix of static and dynamic VAr injection. System performance criteria regarding the amount of voltage dip following a disturbance, duration of voltage dip and post transient voltage recovery level were set. Then multiple contingency screening was performed. Multiple contingencies were limited to N-1-1, a unit and a line outage. Then static steady state and dynamic analysis were performed to investigate the voltage levels. As part of the static analysis, power flow and PV

studies were performed to investigate thermal problems and determine load serving capability. Dynamic analysis was used to study fast voltage collapse phenomenon and perform load sensitivity studies. Severe contingencies were chosen according to the voltage dip level as well as the extra amount of reactive power generators had to provide during the post contingency period. After choosing the most severe contingency the amount of additional reactive power provided by nearby generators is considered as the optimal size of the VAr compensation devices. An iterative dynamic simulation was used to determine the optimal size and location for dynamic devices considering physical size, cost, and short circuit strength of the substations. After determining the size and location of dynamic devices, Optimal Power Flow (OPF) was used to come up with the size and location of static shunt compensation.

OPF is also used in [5] to solve particular contingencies which lead to divergence in a classical Newton-Raphson power flow algorithm, which indicates reactive power deficiency in the system. The OPF is provided with certain constraints, such as allowable voltage levels and the range of VAr injection amounts. The OPF will typically provide the optimal locations and sizes for VAr injection devices that satisfy the given constraints. However, QV and PV analysis are suggested to be used to confirm the OPF results and refine the proposed solution. Extensive load sensitivity analysis in time domain is then used to determine a prudent mix of dynamic and static VAr resources, and to ensure that the optimal allocation and sizing of VAr injection devices are effective for system transients as well as steady state conditions.

Therefore, static methodologies in general and specifically OPF studies have been the main tools in determining the optimal location and size of VAr injection devices. Dynamic VAr injection devices are optimized using time simulations iteratively to either validate or modify the results obtained from the static studies. However, in contrast to the previous approaches this work uses dynamic time domain analysis as the tool to evaluate the voltage sensitivities of load buses during contingencies, and then these sensitivities are used to optimize the size and location of dynamic VAr devices.

1.3 Thesis Organization

This thesis is comprised of six chapters.

Chapter 2 introduces load modeling concepts and explains the various characteristics of load types and their effect over voltage stability. The importance of dynamic load modeling in capturing the system dynamics is also presented in this chapter. The development process of composite load model and its characteristics are discussed as well.

Chapter 3 gives a brief introduction to voltage stability issues and their impact on power system overall reliability. Short term voltage stability and fast voltage collapse are identified, and the effect of load dynamic behavior on these issues is also presented. The last part of this chapter is dedicated to voltage instability counter-measures and the use of VAr injection dynamic devices.

Chapter 4 presents the proposed methodology used in this work to perform the dynamic optimization process. The role of voltage trajectory sensitivities in the optimization problem and the procedure for calculating them are explained as

well. An approach to determine the optimal VAr injection values is also introduced.

Chapter 5 is devoted to simulation results. It also presents the values of voltage trajectory sensitivities and optimal VAr injection values for different operating conditions for the IEEE test system considered. This chapter includes plots for the load voltage response for each case.

Chapter 6 presents the conclusions for the results of this work and suggests the direction for further research.

CHAPTER 2

LOAD MODELING

2.1 Introduction

Loads in transient stability studies are generally defined as active power consuming devices connected to the power system at bulk power delivery points. These devices are formed by aggregating a large number of load components and representing them as a single entity [6, 7]. A load model is a mathematical representation that takes the voltage and possibly frequency as inputs, and gives the load active and reactive power consumption as its output [8]. In traditional power flow and steady state analysis studies a single mathematical model that describes the behavior of these load components is assigned for each load aggregation. This grid-level approach has greatly reduced the complexity associated with representing load in power system studies and made it possible to perform these computer studies within reasonable time and with acceptable accuracy [1].

However, with the growing complexity of load behavior which results from introducing new and more sophisticated load components, such as: solid state electronic devices, discharge lighting, control and protection technologies, motors, and other relevant devices the grid-level representation approach previously mentioned appears to be missing out a significant amount of important details for the sake of simplifying the behavior of large number of different load devices into one single mathematical model. This negative aspect has started to surface in the form of inconsistency between simulation results using these simplified load models and the actual -measured- behavior of the system for certain

events, especially the incapability of reproducing delayed voltage recovery events [6, 9, 10, 11].

Since computer simulations are the most important -and sometimes the only- tool used for planning and operation purposes, a different load representation that would lead to higher accuracy levels is needed [12]. This concern is magnified by the fact that power systems operating conditions are also changing and moving towards the edge of operational stability in order to satisfy the growing demand and to maximize profits [8]. Therefore, accurate studies are needed to avoid possible costly outages and/or damages.

Despite the research conducted in the field of load modeling and the improvements achieved, it is still considered a challenging and non-trivial problem due to the nature of loads which can be described by the following [6, 8, 9]:

- Large number of load components with highly diverse characteristics and behavior
- Load composition and magnitude are constantly changing with time. The scope of time change here is within day, week, month season, and due to weather. This introduces a statistical characteristic for actual loads which makes it difficult to represent using deterministic methods.
- Lack of data describing the load since most of the load is located at the customer side which makes it inaccessible to electric utilities.
- Lack of dynamic measurements. This is because artificial disturbances initiated by utilities such as changing transformers tap, are too small to

reveal the discontinuous nature of load, and uncontrolled large disturbances could take place outside the loading conditions of interest.

- In the distribution system, loads are connected with a myriad of continuous and discrete control and protection devices, which affect the load behavior significantly under voltage and/or frequency disturbances.

2.2 Load Model Requirements

Before proceeding to the development of new load models, the requirements expected from these models should be determined. These requirements are extracted from the need for results with high accuracy levels for simulations and power system studies such as transient and short term voltage stability analysis and other static and dynamic studies. A successful and effective load model should be able to [1, 8]:

- Capture and reproduce the behavior of aggregated load components when subjected to practical variations in system voltage and/or frequency with an acceptable accuracy. This includes the ability of representing voltage recovery delays, voltage collapse, oscillations, etc. in both transient and steady state time frame.
- Represent rotating loads (motors) dynamically, which makes it capable of capturing motor stalling conditions and their impact over voltage recovery. It should also capture the sensitivities of motor real and reactive power requirements with respect to applied voltage.

- Represent the effect of components lost in the lumped loads such as: thermal protection devices, under-voltage contactors, distribution transformers and feeders, shunt capacitors, etc.

However, the load model should not be overly complex or cause simulations to become a computational burden. The model should also be physically based, which makes it possible to derive the load model and modify it using information which is relatively easily obtained [8].

2.3 Present Load Modeling Practices

As mentioned before, successful and effective load model essentially aggregates load from component-level to grid-level without losing the details needed to capture the behavior of these individual components [1, 8]. Three major approaches have been used to achieve the required data needed to build load models. These approaches are [6, 8, 9, 13]:

- Simplified voltage dependant models
- Measurement based modeling
- Component based modeling

The following subsections briefly explain each of these approaches.

2.3.1 Simplified voltage dependant models

This approach is relatively simple because it depends on engineering judgment and knowledge, and it also lacks any explicit dynamic presentation. Load in this approach is divided into three different static models depending on how it is assumed to respond to system perturbation in voltage and/or frequency [6, 7, 13]:

- Constant power load model: loads governed by this model are assumed to consume a constant amount of active and reactive power all the time even with voltage variation, such as motors and electronic devices. However, it should be noted that most constant power devices will not retain this behavior below a certain level of voltage. For example, a motor may stall at voltages below 60% [14] and change into a constant impedance model. Loads may also be tripped at low voltages. This makes the constant power load model valid for limited conditions.
- Constant current load model: the power consumption of loads in this model varies directly with voltage magnitude. Resistive heating and lighting loads are usually described by this model.
- Constant impedance load model: loads governed by this mode are assumed to change their power consumption directly with the square of voltage magnitude. Incandescent lighting, stalled motors and the reactive power part of rotating loads are usually described with this model.

Although models are easily built and used in this approach, the lack of dynamic representation for rotating loads, and the lack of empirical justification for this approach make its accuracy unacceptable for transient and voltage stability analysis [8].

2.3.2 Measurement Based Modeling

Data are obtained for this approach of modeling by installing measurement and data acquisition devices such as: power quality monitors, PMUs and dynamic event monitors. at load buses and feeders. These devices are used to measure and

record the change in active and reactive power consumption with respect to the deviation in voltage and frequency [6, 8, 13]. The perturbation could be artificial such as changing a transformer tap or switching a shunt capacitor, or natural as a real disturbance. The collected data is then fitted into a mathematical model representation. In [13] it is suggested to use the non-linear least-squares method as a suitable algorithm for this approach.

The obvious advantage of this approach is the use of real data with physical origin as the basis for developing the load model. However, this approach has the following shortcomings [6, 8, 13]:

- The produced model is only valid for the load composition at the load bus or feeder where the measurements were taken.
- The produced model is only valid for the particular time of measurement (i.e. time of the day, day of the year and season
- If the measurements were based upon artificial perturbations, this means the produced model is only valid for small disturbances (5% - 7%). This disadvantage is particularly relevant to rotating loads behavior, making it impossible to develop a dynamic model that describes the nonlinearities and discontinuous behavior of models at significantly low voltages.

2.3.3 Component Based Modeling

In this approach load components are aggregated into groups according to their nature of use, these groups are called classes. The used classes for this approach are: residential, commercial, industrial and agricultural [6, 8, 9]. This cate-

gorization reduces the variability in load characteristics between different locations. Then for each class certain sets of components are assumed to be present to form the load composition for that specific class. The characteristics for these components are decided individually using theoretical analysis or laboratory measurements. Figure 2.1 explains how the categorization is performed.

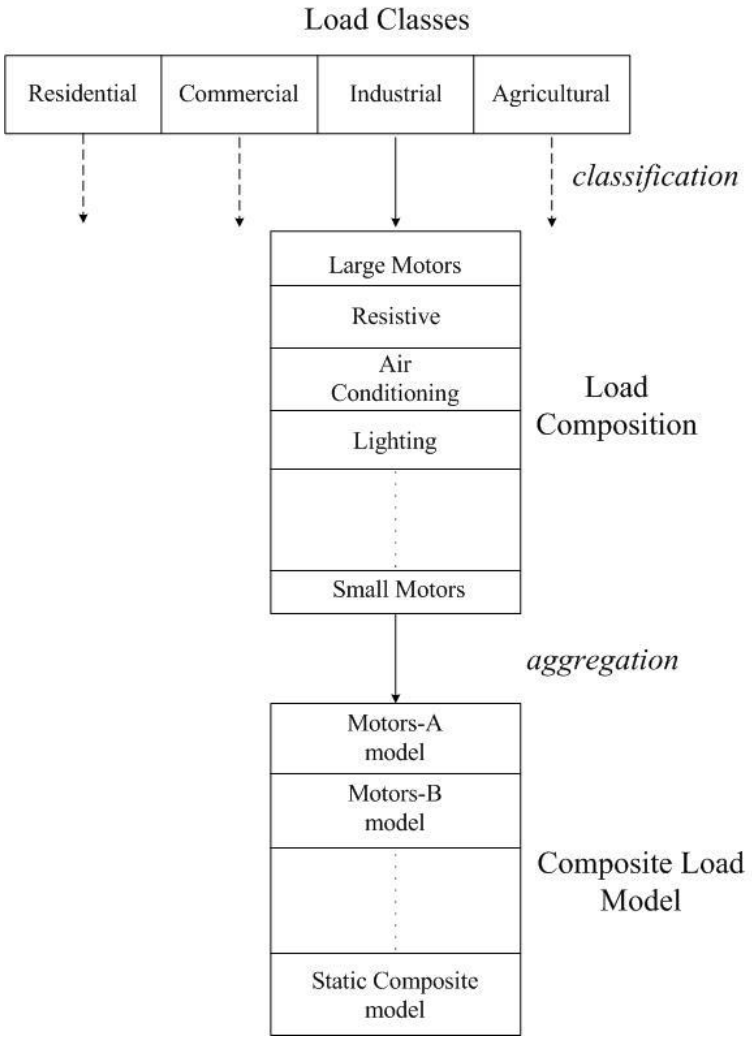

Figure 2.1 Component based modeling

This approach has the advantage of being more realistic than the measurement method because it has the flexibility of including all types of loads explicitly, including dynamic behavior of rotating loads.

However, this approach has a major drawback which is the need for data describing the present class mixes and components included in each mix. This can be achieved by thorough surveys from various utilities.

2.4 Static Composite Load Model (ZIP)

From the previous discussion it is obvious that more than one single static load model is needed to describe the behavior of load aggregation. This is due to the fact that different load components with different characteristics were embodied into a single entity [6, 7, 13]. Static composite load model was developed to represent the complex relation between power and voltage magnitude through an algebraic relation that combines the three different static load models (constant impedance *Z*, constant current *I*, constant power *P*), hence it is sometimes called ZIP model.

A polynomial equation is usually used to represent the composite static model as follows:

$$P = P_0\left(P_1\left(V/V_0\right)^2 + P_2\left(V/V_0\right) + P_3\right)\left(1 + a_{pf}\Delta f\right) \tag{2.1}$$

$$Q = Q_0\left(Q_1\left(V/V_0\right)^2 + Q_2\left(V/V_0\right) + Q_3\right)\left(1 + a_{qf}\Delta f\right) \tag{2.2}$$

where V_0 is the rated (or initial) voltage, P_0 and Q_0 are the active and reactive power, respectively, consumed at V_0. P_1, P_2 and P_3 are coefficients that specify the portions of load of which their real power corresponds to constant impedance,

constant current and constant power respectively. The summation of these coefficients equals 1. The terms Q_1, Q_2 and Q_3 are the reactive power corresponding coefficients. It can be noticed that a frequency dependency linear term has been added to both equations to capture frequency change effect over power consumption response. Δf is the deviation in frequency from nominal value, a_{pf} and a_{qf} are the frequency sensitivity of active and reactive power respectively.

The polynomial model has limited flexibility in representing highly voltage sensitive and nonlinear loads. For example the reactive power of discharge lighting is proportional to voltage to the power four [15]. Therefore, an exponential model which provides more flexibility can be used. The exponential composite static model is as follows:

$$P = P_0\left(P_1\left({}^{V}/_{V_0}\right)^{P_{e1}} + P_2\left({}^{V}/_{V_0}\right)^{P_{e2}} + P_3\right)\left(1 + a_{pf}\Delta f\right) \tag{2.3}$$

$$Q = Q_0\left(Q_1\left({}^{V}/_{V_0}\right)^{Q_{e1}} + Q_2\left({}^{V}/_{V_0}\right)^{Q_{e2}} + Q_3\right)\left(1 + a_{qf}\Delta f\right) \tag{2.4}$$

It can be noted that the exponential form is more general than the polynomial one, since by assigning the exponentials P_{e1} and P_{e2} the values 2 and 1 respectively the polynomial model can be realized.

2.5 Motor Modeling

Rotating loads which include all the different types of motors are responsible of the dynamic behavior loads have during transients. Previous discussed static models are not able to capture these dynamics due to the high nonlinearity and discontinuity in motors behavior under depressed voltage levels. Motors can occupy around 72% of the total load [16], especially in areas with summer load

peak where air conditioners (A/C) are intensively used. Most of the industrial load is also comprised of motors. In the case of certain industrial loads motors can represent around 98% of the total load [17].

With this high motor load penetration, dynamic behavior becomes very significant and important to capture in transient studies, especially in short term voltage stability analysis. Voltage recovery delay -or even collapse- following a fault is directly related to decelerating and stalling motors as will be explained next. Two types of motors will be discussed:

- Three phase induction motors
- Single phase A/C motors

Those two types were chosen because they are the most commonly used motors, and have the largest impact over voltage stability [7, 10].

Three phase induction motors

The key factors in determining a motor active and reactive power response to voltage variations are the inertia (motor and load shaft inertia) and rotor flux time constant [6]. Therefore, it is desirable to differentiate between large and small induction motors according to their inertia, since motors with low inertia tend to decelerate and stall faster than large motors.

In steady state operation, the motor electrical torque is equal to the mechanical torque of the mechanical load connected to it. However, under voltage disturbance (usually depressed voltage magnitude due to a fault) the generated electrical torque is reduced depending on the voltage magnitude, since the electrical torque is proportional to the voltage squared. This state of non-equilibrium

between electrical and mechanical torque will cause the motor to decelerate. The deceleration rate depends on the applied voltage level and on the mechanical load characteristics. Mechanical load torque can be either speed dependant (fans, pumps, etc.) or constant (reciprocating and rotary compressors), naturally constant torque will cause higher deceleration rate. During deceleration the slip will proportionally increase causing the motor to draw high current at low power factor. The increased consumption of reactive power is responsible for delaying the voltage recovery and can even cause a voltage collapse. If the fault is not cleared promptly, and there is not enough reactive power, motors will decelerate till they stall. Figure 2.2 shows typical torque and current characteristics for an induction motor.

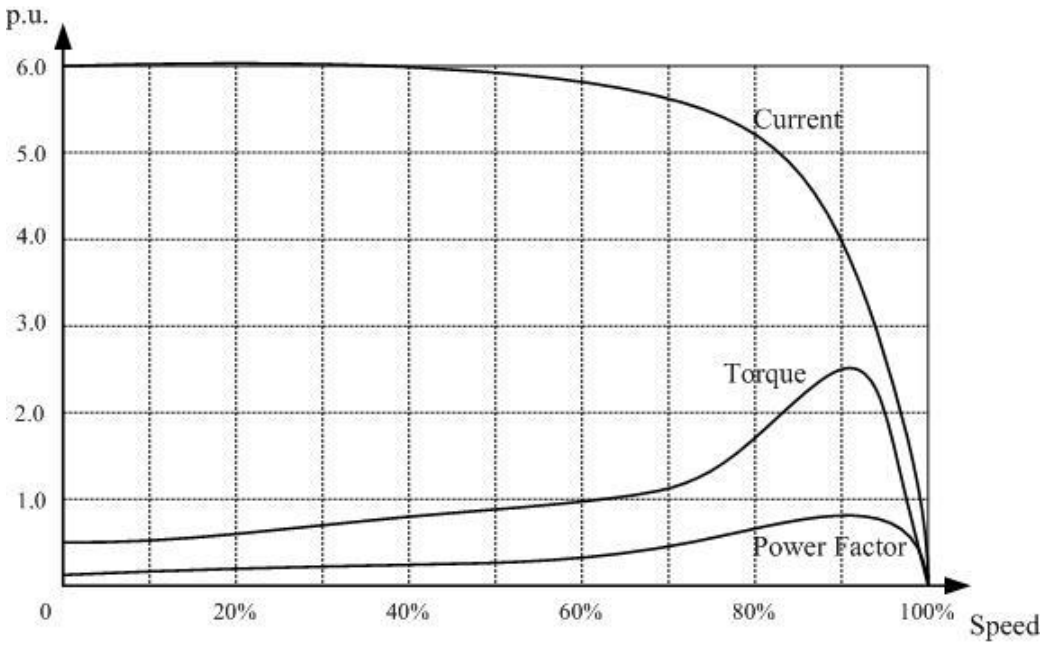

Figure 2.2 Induction motor torque and current curves

2.5.1 Induction Motor Modeling

To capture the previously mentioned phenomena associated with induction motors, a dynamic model is required. Three models that describe induction motor exist [13]:

- First order induction motor model: a purely dynamic mechanical model that neglects internal electric dynamics.
- Third order induction motor model (single cage rotor model): includes rotor flux dynamics along with mechanical dynamics.
- Fifth order induction motor model (double cage rotor model): includes mechanical dynamics, rotor flux dynamics and stator flux dynamics.

The third order model is usually used for its capability of capturing mechanical and electrical dynamics with moderate complexity. The stator flux transient response is very fast compared to rotor flux response and the transient state of the power system, which makes neglecting it possible [13]. Figure 2.3 shows the equivalent circuit of a single cage rotor motor in steady state.

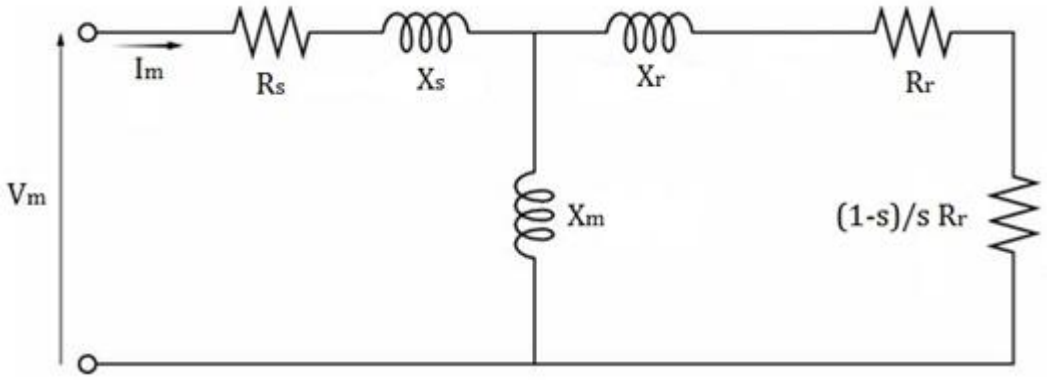

Figure 2.3 Single cage rotor IM equivalent circuit

2.5.2 Single Phase A/C Motor

The dominant power consuming part of the single phase air conditioner units is the compressor motor, it consumes up to 87% of the total unit consumption [9]. Therefore, this type of motors have to be modeled and considered in transient studies, especially in areas which have summer load peaks. Single phase A/C motors are prone to stall because of their low inertia and the mechanical characteristics of the compressor they drive [11, 14], therefore, they are directly responsible for the delayed voltage recovery phenomenon. Under stall conditions (i.e. slip=100%) motors draw very high current with a very low power factor, the amount of this current is only determined by motors rated locked-rotor current and the applied voltage. In some cases this current can be as high as 8.5 p.u. for residential A/C [14]. Similar to induction motors, under reduced voltage conditions the electrical torque will start to drop down causing the motor to decelerate. The motor will continue to decelerate until it is unable to overcome the pressure applied by the compressor, at this point the motor stalls. Usually single phase A/C motors stall if the voltage falls to between 50 – 65 % of nominal voltage for more than 3 cycles [15]. Stalling voltage depends on other factors, such as: ambient temperature and humidity. Figure 2.4 shows the reactive power consumption of a stalled A/C motor.

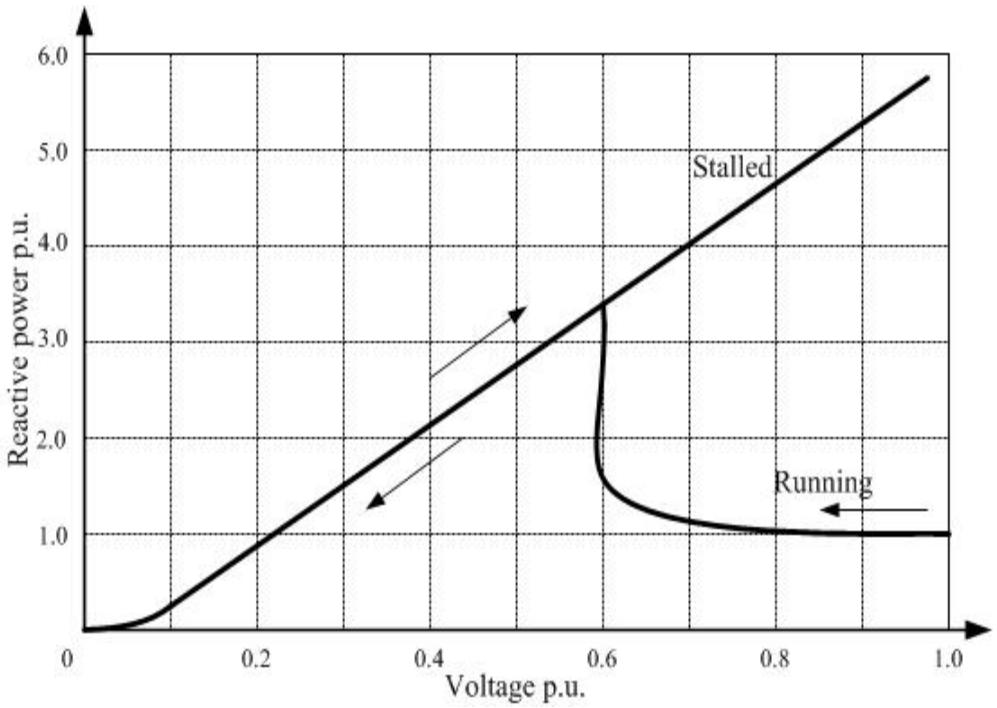

Figure 2.4 Reactive power consumption for a stalled

single phase induction A/C motor

Stalled A/C motors can in some cases re-accelerate if the voltage recovers to a certain level (roughly above 70%). However, re-accelerating after stall condition depends on the type of compressor connected to the motor. Laboratory tests show that for scroll compressors re-accelerating is possible while it is not the case for reciprocating compressors [15].

Single phase A/C motors are also equipped with under-voltage and thermal relays which should be included in the model since they significantly affect the dynamic behavior of these motors. Thermal relays usually operate in response to the high current drawn during stall conditions. The time required for thermal relays to operate depends on the drawn current. Usually a stalled motor will be tripped by thermal protection relay after 3 – 30 seconds (depending on the current

magnitude). Thermal tripping could happen for an individual unit or for a whole feeder that is supplying many stalled motors. Under-voltage protection contactors operate faster than thermal ones, actually under-voltage contactors open almost instantaneously at low voltages (35 – 45 %), and can reclose at voltages above 50% [9].

2.5.3 Single phase A/C motor modeling

The characteristics of single phase A/C motors discussed above have significant impact on short term voltage stability analysis and must be included in the model. The controls and protection schemes should also be included in the load model since they control tripping and reconnecting the units. Laboratory tests and offline simulations have proved that three phase induction motor model is not adequate to capture the dynamic response of single phase A/C motors [1], especially the stalling conditions. However, the steady state behavior of both motors is very similar and a three phase induction motor can be suitable to capture the behavior of single phase A/C motor in steady state conditions. To include the stalling conditions, a fictitious shunt component is connected in parallel with the motor to replace it with the locked-rotor impedance representing a constant impedance model. This approach is called "hybrid performance based modeling" [15].

2.6 Composite load model structure

The Western Electricity Coordinating Council (WECC) developed an interim composite load model that was used for planning and operation studies in early 2002 [9]. This model was represented by 80% of load as static, and 20% as induction motor load. This interim model was unable to represent delayed voltage

recovery events following a major transmission fault. Simulations using this interim model indicated instantaneous voltage recovery contrary to the real recorded event. Therefore, WECC formed a load modeling task force (LMTF) to improve the interim model and develop a more accurate and comprehensive one. The LMTF acknowledged the following factors in the improved composite load model:

- The electrical distance between the point where the load is connected in simulations (usually transmission or sub-transmission level) and the point where the physical load is connected (distribution level). Therefore, the improved model will include the network components such as: feeders and transformers impedance, shunt devices, protection, transformer taps, etc.
- Single phase A/C motors have very significant impact over voltage stability and should be included in the new model explicitly since the induction motor model is not adequate to represent their characteristics. This will allow the new composite model to capture the dynamic behavior of these motors such as: decelerating, stalling, tripping, etc.
- Induction motors vary widely in characteristics depending on size, number of phases and mechanical torque they drive. Therefore, the new model should differentiate between the different types of induction motors. This provides more flexibility and accuracy in representing motor loads.

Figure 2.5 shows LMTF proposed composite load model.

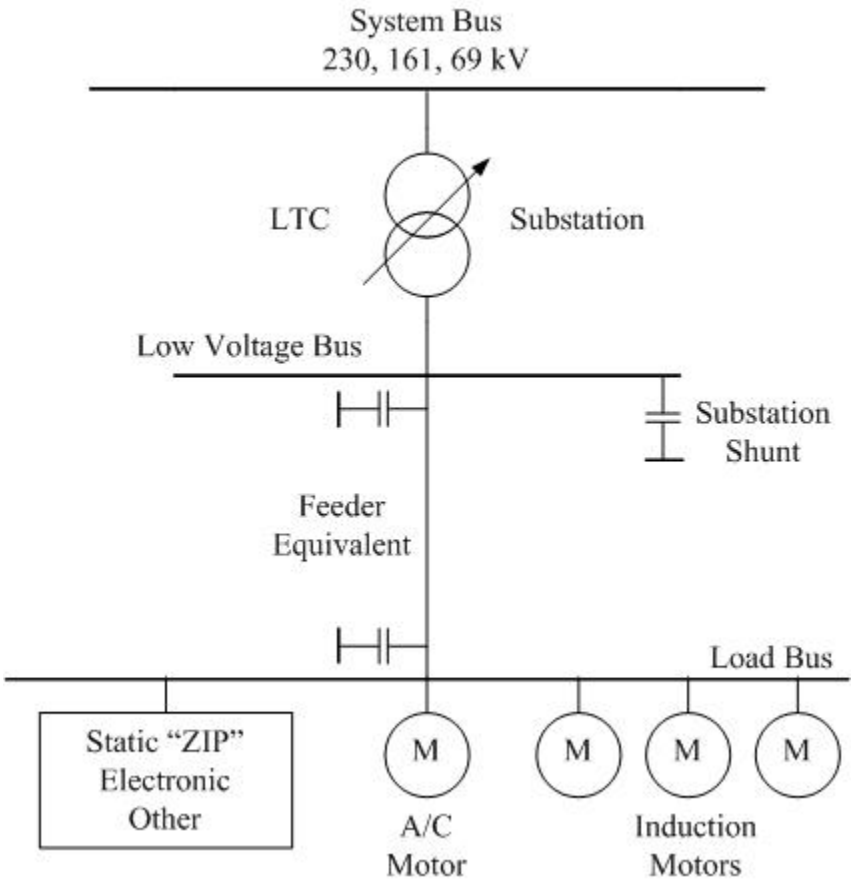

Figure 2.5 LMTF proposed composite load model

CHAPTER 3

VOLTAGE STABILITY AND VAR COMPENSATION

3.1 Introduction

Voltage stability is the ability of a power system to maintain steady acceptable voltages at all buses in the system under normal operating conditions and after being subjected to a disturbance [18]. Disturbances could be large such as major transmission faults, generating unit tripping, loss of major components or small such as a gradual change in load. Voltage instability occurs when one system bus -or more- suffers from progressive and uncontrolled change in the voltage magnitude, usually in the form of voltage decrease. Voltage instability can cause prolonged periods of voltage depression conditions (brownout), or even a voltage collapse and blackout depending on the available reactive power and load dynamics. Although voltage instability is essentially a local phenomenon, however voltage collapse which is more complex than simple voltage instability and is usually the result of a sequence of events, is a condition that affects large areas of the system [18].

Rotor (angle) stability had been the primary aspect of stability studies for decades. However, recent events of abnormal voltage magnitudes and voltage collapse incidents in some large interconnected power systems have sparked the interest in the voltage stability phenomenon [2, 19]. Rotor stability was believed to be responsible of voltage instability conditions. This case is true since a gradual loss of synchronism of machines as rotor angles between two groups of machines approach or exceed 180° would result in very low voltages at intermediate points

in the network. However, this is not the case if the disturbance was close to load centers and the voltage depression was rather caused by load dynamics and reactive power deficiency. Therefore, voltage instability may occur when rotor stability is not an issue. Actually, sustained voltage instability conditions can cause rotor instability [18].

Several recent factors and operating conditions have also caused the voltage instability problem to become more prevalent, such as [20, 21]:

- Power systems in general and specifically transmission lines tend to be operated under more stressed conditions. This stressed operating condition is not only due to continuous and significant load growth, but also because of major changes and restructuring of energy markets. Stressed transmission lines have less capability of delivering reactive power to demanding load centers because of the high reactive power losses. Transmission lines (especially long ones) with relatively large voltage angle difference between sending and receiving ends also have limited capability of reactive power delivery.
- High rates of induction and single phase motor penetration, especially those used in air conditioning systems, heat pumps and refrigeration. These motors are known as low inertias machines, as a result they have fast response to disturbances. Voltage instability issues are directly related to dynamic behavior of motors.
- Electronic loads which have significant discontinuous response to variations in voltage magnitude.

- The use of HVDC tie lines to transfer large amounts of electric power. The convertors associated with these lines consume significant amounts of reactive power.
- Excessive reliance on shunt connected capacitor banks for reactive power compensation. In heavily shunt capacitor compensated systems, the voltage regulation tends to be poor. Another disadvantage for shunt capacitors is that the reactive power support they provide is directly proportional to the square of the voltage. Therefore, at low voltage when the reactive power support is most needed, the VAr output of the capacitor banks drops.

3.2 Classification of Voltage Stability

It is useful to classify voltage stability into subclasses in order to better understand the system behavior under voltage instability conditions. Classification also helps choosing the right analytical strategies depending on the nature of the phenomenon of interest. Voltage stability is classified here according to the magnitude of the disturbance affecting the system into two subclasses [18]:

- Small disturbance voltage stability: also called small-signal or steady-state voltage stability. This type of voltage stability is related to small and possibly gradual perturbations in the system, such as small changes in the load. Small-signal stability is determined by the characteristics of load and continuous and discrete controls at a specific instant of time. A criterion for this type of voltage stability is that at a given operating condition, for every bus in the system, the bus voltage magnitude in-

creases as the injected reactive power at the same bus is increased. When analyzing small disturbance voltage stability usually either mid-term (10 seconds to few minutes) or long-term (few minutes to tens of minutes) studies are performed.

- Large disturbance voltage stability: also called transient voltage stability. Large disturbance here refers to major changes in operating conditions. These changes could be major faults on transmission lines, generating units tripping, transmission lines tripping, or other large disturbances. The transient voltage stability is determined by the load characteristics, continuous and discrete controls, as well as the protection systems. However, in order to capture the nonlinear dynamic interactions between the different system components and their effect on transient voltage stability, a dynamic time domain analysis should be performed. This type of analysis is referred to as short-term voltage stability analysis (0 to 10 seconds). A criterion for large disturbance voltage stability is that following a large disturbance and after the actions of system control devices, voltages at all buses reach acceptable steady state levels.

3.3 Voltage Stability Analysis

From the previous discussion it is apparent that each subdivision of voltage stability has its own characteristics and nature, therefore each type has to be approached and analyzed using the appropriate analytical tool. In general, voltage stability problems are studied by two approaches [18, 22]:

- Static analysis
- Nonlinear dynamic analysis

3.3.1 Static Analysis

Static analysis studies are used for steady state voltage stability problems initiated by small disturbances. The system dynamics affecting voltage stability in the event of small disturbances are usually quite slow and much of the problem can be effectively analyzed using the static approaches that examine the viability of a specific operating point of the power system [18]. Power flow is used for this type of study, where snapshots are captured from different system conditions at certain time instants. At each of these time frames system dynamic equations are linearized, and time derivatives of the state variables are assumed to be zero, while state variables take their numerical value at that time instant. Therefore, the resultant system equations are simple algebraic equations that can be solved using power flow simulation.

Static analysis can be performed faster than dynamic simulations and needs less modeling details. However, with the presence of fast acting components such as motors, and HVDC convertors, the dynamic effect and the interactions between controllers and protection must be included in the voltage stability analysis to capture the actual behavior of the system [18, 23].

Steady state static studies are not only useful in the determination of the voltage stability of a given operating conditions, but they also provide information about the proximity of these conditions to voltage instability, as well as voltage sensitivity. Static analysis has been solved by different approaches [18, 23]:

V-Q sensitivity analysis: The linearized region provided by power flow analysis around a given point is used to indicate the relation sensitivity between the voltage and reactive power. This sensitivity is described by the elements of the Jacobian matrix. The power equation equations (polar form) for any node *i* can be written as

$$S_i = P_i + jQ_i = V_i I_i^* \tag{3.1}$$

where, S_i, P_i, Q_i is the complex, real and reactive power injections at bus *i* respectively. The term V_i is the bus voltage, and I_i^* is the conjugate current injected at bus *i*.

Power flow equations (real form) of bus *i* with respect to the rest of the system are written as

$$P_i = V_i \sum_{m=1}^{n} (G_{im} V_m cos\theta_{im} + B_{im} V_m sin\theta_{im}) \tag{3.2}$$

$$Q_i = V_i \sum_{m=1}^{n} (G_{im} V_m sin\theta_{im} - B_{im} V_m cos\theta_{im}) \tag{3.3}$$

where, *G* and *B* are the real and imaginary parts of the admittance matrix respectively. θ_{im} is the voltage angle difference between buses *i* and *m*. The Jacobian matrix is used to achieve the following linearized form

$$\begin{bmatrix} \Delta P \\ \Delta Q \end{bmatrix} = \begin{bmatrix} J_{P\theta} & J_{PV} \\ J_{Q\theta} & J_{QV} \end{bmatrix} \begin{bmatrix} \Delta\theta \\ \Delta V \end{bmatrix} \tag{3.4}$$

where, $\Delta P, \Delta Q, \Delta\theta, \Delta V$ are the incremental changes is bus real power, reactive power injection, voltage angle and voltage magnitude respectively. Although system stability is affected by the real power, it is possible to keep *P* constant in or-

der to evaluate the sensitivity only between the reactive power and voltage magnitude. Therefore by setting $\Delta P = 0$

$$\Delta Q = J_R \Delta V \tag{3.5}$$

where J_R is the reduced Jacobian matrix of the system and can be written as,

$$J_R = [J_{QV} - J_{Q\theta} J_{P\theta}^{-1} J_{PV}] \tag{3.6}$$

The *V*-*Q* sensitivity at a bus represents the slope *Q*-*V* curve at a given operating point. A positive value for the sensitivity indicates stable conditions. The larger the sensitivity index the closer is the operating point to instability. The value of infinity represents stability limit or the critical point. Negative values for sensitivity indicate unstable conditions, with very small negative values representing highly unstable conditions.

Q-*V* modal analysis: This analysis approach has the advantage of providing the mechanism of instability at the critical point. The eigenvalues and eigenvectors of the reduced Jacobian matrix are evaluated and used to indicate voltage stability. Positive eigenvalues represent stable voltage conditions, and the smaller the magnitude, the closer the relevant modal voltage is to being unstable.

Compared to *V*-*Q* sensitivity analysis, *Q*-*V* modal analysis is more capable of identifying the voltage stability critical areas and elements which participate in each mode once the system reaches the voltage stability critical point, hence, it can describe the mechanism of voltage instability. *V*-*Q* sensitivity analysis is not able to identify individual voltage collapse modes; instead they only provide information regarding the combined effects of all modes of voltage-reactive power variations.

V-Q curve analysis: *V-Q* curves show the relationship between the reactive power support at a certain bus and the voltage of that same bus. For large power systems these curves are obtained by a series of power flow simulations. A fictitious synchronous condenser with unlimited reactive power capability is placed at the test bus, and the voltage magnitude is varied through the simulation [24].

V-Q curves are useful in determining the amount of reactive power needed to be injected at a certain bus in order to obtain a desired voltage level. Therefore, these curves can be used for both; voltage stability indication purposes, and shunt compensation sizing. However, it should be noted that *V-Q* curves are only valid for steady state analysis [2]. It should also be noted that power flow equations tend to converge around the voltage stability critical point, therefore, special techniques have to be used to overcome the divergence problem, such as continuation power flow.

3.3.2 Nonlinear Dynamic Analysis

Dynamic analysis provides the most accurate results for voltage stability phenomenon using time domain simulations which capture the real dynamic nature of the system without any approximations. Nonlinear dynamic simulation is therefore very useful and effective for short term voltage stability studies and fast voltage collapse situations following large disturbances [22]. However, as a price for this accuracy, dynamic simulations are much more complicated than static studies since the overall system equations include first-order differential equations that have to be solved as well as the regular algebraic equations. Solving these equations requires significant computational capacity and is relatively time con-

suming. Dynamic simulation results accuracy depends mainly on the models used, therefore, system components have to be modeled in details and with high accuracy [18].

The system set of differential equations can be expressed as follows:

$$\dot{x} = f(x, V) \tag{3.7}$$

And the set of algebraic equations as:

$$I(x, V) = Y_N V \tag{3.8}$$

where, (x_o, V_0) are the initial conditions, x: state vector of the system, V: bus voltage vector, current injection vector, Y_N: bus admittance matrix.

Although no expression for time appears explicitly in the previous equations, however, Y_N is a function of both voltage and time since certain time varying components such as transformer tap changer, phase shift angle controls, etc. are included in it. Also, the relation between I and x can be a function of time [18]. Numerical integration alongside with power flow analysis is usually used to solve the nonlinear dynamic equations in the time domain.

3.4 Reactive Power Support Measures

The previous discussion illustrates the direct effect reactive power has over voltage magnitudes and consequently over the overall system voltage stability. A fundamental aspect of controlling the voltage levels throughout the system is reactive power balance, and hence compensation is considered. Depending on the operating conditions, system components could be either absorbing reactive power, such as: loads in general and heavily loaded transmission lines, or supplying reactive power, such as: underground cables or transmission lines with very

light load. However, since the usual issue with voltage stability is under-voltages (as a result of disturbances) and heavily stressed transmission lines, reactive power injection is usually needed. It should also be noted here that reactive power compensation increases the active power transfer capabilities, and reduce the system losses (increase efficiency). Several techniques are used as reactive power compensation measures, such as [18, 24]:

- Synchronous condensers
- Series capacitors
- Shunt capacitor banks
- Shunt reactors
- Static VAr systems.

3.4.1 Synchronous Condensers

A synchronous condenser is a synchronous machine running without a prime mover or mechanical load, usually in over-excitation mode [18]. The amount of reactive power supplied (or absorbed) by this machine is controlled by controlling the field excitation current. Synchronous condensers need to be supplied with small amounts of active power to supply losses, and they are considered as active shunt compensators. Synchronous condensers have the following advantages:

- Instantaneous response to voltage variations.
- The ability of producing constant reactive power regardless of the system voltage level.

- Their maximum output reactive power limits can be exceeded for certain period of time.

However, synchronous condensers main disadvantage is their high initial and operating costs.

3.4.2 Series Capacitors

Series capacitors can be connected either to distribution feeders or high voltage transmission lines [18]. However, series capacitors are more commonly used in high voltage transmission lines because of the long distance of these lines. Series capacitors are used to reduce the net transmission line inductive reactance and therefore they reduce the reactive power losses through the line, and increase active power transfer capabilities, as well as improving transient stability [24]. Since they are connected in series with the line reactance, the reactive output power of series capacitors is self regulated and is proportional to the square of the current. Therefore, series capacitors output reactive power will increase at high load currents when it is most needed almost instantaneously.

However, series capacitors have the following disadvantages and complications:

- Subsynchronous resonance phenomenon.
- Overload for parallel line outages. An outage of one line in a 2 circuit transmission line with almost double the current in the remaining circuit, this will cause the series capacitor to quadruple.
- Overvoltage profiles at one side of the transmission line under high load currents.

3.4.3 Shunt Capacitor Banks

Whether the shunt capacitor banks are installed in the transmission or the distribution network, the main purpose of using them is to improve the lagging power factor and bring it close to unity. Therefore, shunt capacitors provide local reactive power for load centers instead of importing this power from remote sites which increases the system efficiency. Shunt capacitor banks are also useful in allowing nearby generating units to operate near unity power factor, and therefore, maximizing fast acting reactive reserves [24]. Since shunt capacitor banks provide reactive power, they are also used as effective voltage regulators. Shunt capacitor banks are usually located on load buses but can also be installed on distribution feeders for feeder voltage control purposes.

Shunt capacitor banks are usually connected to the system through mechanical switches. These switches can be controlled manually, by under-voltage relays, or by timers. Shunt capacitor banks have the following advantages [18, 24]:

- Low implementation and maintenance cost
- Flexibility in installation and operation
- Require simple control schemes.

However, shunt capacitor banks have the following limitations and disadvantages [18, 24]:

- Output reactive power produced is directly proportional to the voltage squared. Consequently, the reactive power output is reduced at low vol-

tages when it is likely to be needed most (i.e. following a large disturbance).

- Mechanical switching is slow compared to power system transients. As a result, shunt capacitor banks are not capable of improving short term voltage stability (i.e. they cannot prevent motor stalling for example).
- Following a large disturbance, if the affected part of the system was isolated, the stable part may encounter very high over-voltages because of energizing the shunt capacitor banks during the period of voltage decay.

3.4.4 Shunt Reactors

In contrast to shunt capacitor banks, shunt reactors are used to regulate voltage by consuming the excess reactive power in a transmission line, and therefore, preventing over-voltages. Switched shunt reactors can also be disconnected from the system to reserve the available reactive power in the case of depressed voltages.

3.4.5 Static VAr Systems

Static VAr compensators (SVCs) are also shunt connected and used to improve voltage stability by either producing or absorbing reactive power. The term static indicates that SVCs do not contain any moving parts, such as rotating components in synchronous condensers, and mechanical switches in shunt capacitor banks. Instead, solid state switches are used to vary the SVCs net susceptance and consequently the overall output. This feature makes SVCs suitable for transient voltage support because they can respond to voltage variations within few cycles [2, 18]. Static VAr system (SVS) includes SVCs and mechanically switched ca-

pacitors or reactors whose outputs are coordinated in a single shunt connected unit.

The following are the mostly commonly used techniques in achieving a variable susceptance [2]:

- Thyristor switched capacitor (TSC): shunt capacitor banks connected to a bus through a bidirectional thyristor switch. Figure 3.1 shows a schematic representation for (TSC).

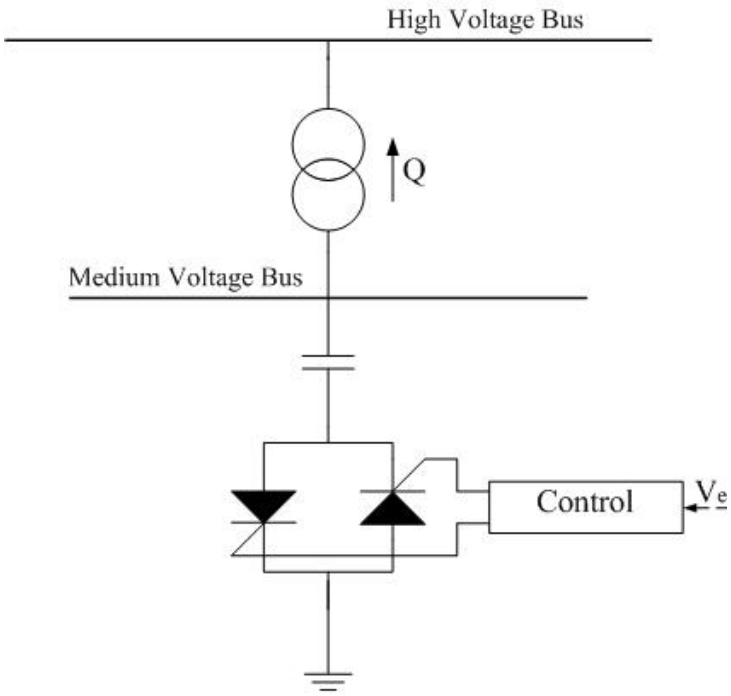

Figure 3.1 TSC schematic representation

- Thyristor controlled reactor (TCR): in this configuration a reactor in series with a bidirectional thyristor switch are connected in parallel with a fixed capacitor, Figure 3.2 shows a schematic representation for (TCR).

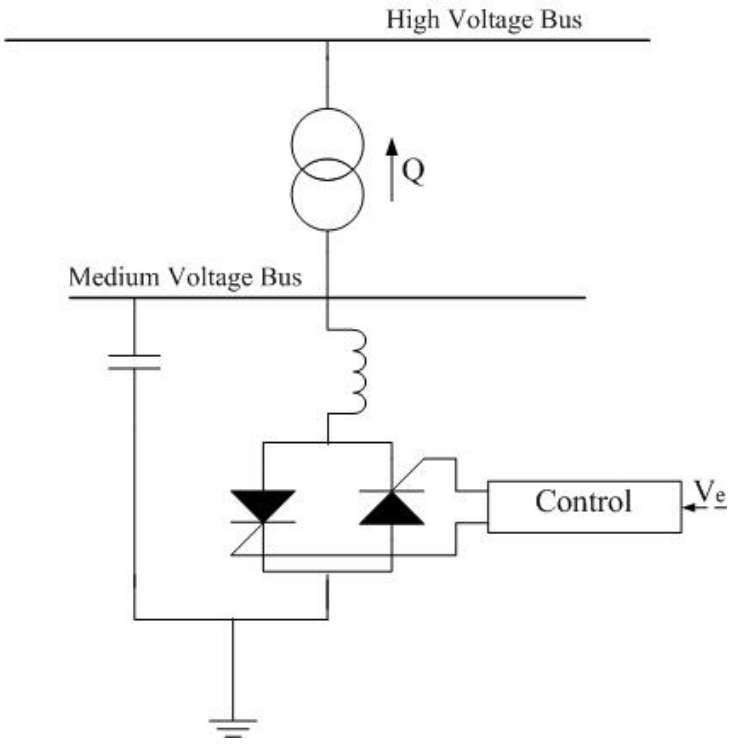

Figure 3.2 TCR schematic representation

In both types the output susceptance is controlled by the firing angle of the thyristors. A controller is used to provide the thyristors with the firing signal depending on the desired output. In steady state operation, the reactive power output of the SVC is:

$$Q = B|V|^2 \tag{3.9}$$

where, V is the bus voltage, and B is the net output susceptance. B can be represented as:

$$B = K|V_0 - V| \tag{3.10}$$

subject to: $B_{min} \leq B \leq B_{max}$

where, K is the SVC gain, V_0 is the reference voltage, V is the actual bus voltage, B_{min}, B_{max} are the minimum and maximum allowed susceptance values, respectively.

At the boost limit, the SVC becomes a fixed shunt capacitor. Therefore, it is desirable to supplement the SVC with mechanically switched capacitors in order to maintain the controllability characteristics of the SVC. Mechanically switched capacitors also help to reset the SVC to its initial set point following a disturbance in order to preserve its output for future operation.

Despite the relatively high initial costs, SVCs have been widely used in power systems because of their fast and precise voltage regulation capabilities which help improving the system transient voltage stability following a large disturbance. As mentioned before, a major disadvantage of SVCs is that at their maximum output they behave as regular shunt capacitors and the reactive power produced is directly proportional to the square of the voltage.

To overcome this problem, a static compensator (STATCOM) is used. Similar to synchronous condenser, STATCOM has an internal voltage source which provides constant output current even at very low voltages. Therefore, the output reactive power of the STATCOM is linearly proportional to the bus voltage. Figure 3.3 shows both, SVC and STATCOM characteristics curves [21].

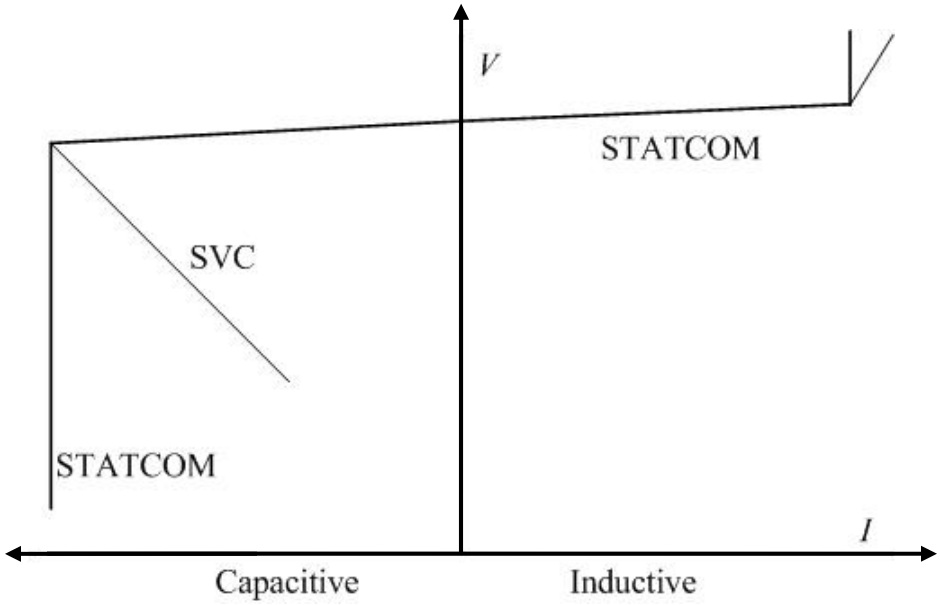

Figure 3.3 SVC and STATCOM characteristic curves

CHAPTER 4

PROPOSED METHODOLOGY

4.1 Motivation

Sufficient reactive power is needed in a power system to achieve normal ac voltage levels to ensure voltage stability. However, if the system is affected by a large disturbance, reactive power consumption will be increased throughout the system and could cause significant depression in voltage magnitudes, especially at load buses. Therefore, reactive power compensation becomes essential to avoid short term voltage instability, or even a fast voltage collapse. The amount of reactive power needed and the instant when this power should be provided become very important in systems heavily loaded with motors and/or any other fast acting dynamic devices. Small motors decelerate very fast with reduced voltages and tend to stall if the ac system voltage does not recover to higher levels promptly. Therefore, the location and amount of VAr compensation should be determined optimally in order to support the short term voltage stability with the least possible cost.

4.2 Objective

The objective of this work is to develop a comprehensive methodology which can determine the optimized VAr compensation (location and level) that is needed to maintain the system short term voltage stability, following a large disturbance close to load centers. This approach should be valid for a range of operating conditions and contingencies. In contrast to previous approaches, this work evaluates the reactive power needs dynamically and in the transient time frame.

4.3 Static Analysis

In order to illustrate the method of reactive power optimization, this work uses a 162-bus, 17-generator, IEEE test case as the base case. A contingency scan was performed by applying a three phase fault at different 345 kV buses. Since short term voltage stability and delayed voltage recovery are directly related to load behavior, the faults were applied at buses close to load centers, and the voltage levels of load buses were monitored. Each fault was cleared after 6 cycles by opening a 345 kV line. The fault that caused the deepest voltage dips at load buses was chosen as the most severe contingency and used in the dynamic simulation. The loads that were most affected by that contingency were chosen to be assigned dynamic load models. These load centers were also stepped down through distribution transformers from the 69 kV voltage level to 12.47 kV. Representing loads in the distribution level provides the opportunity to include network effects and achieve more accurate results.

4.4 Dynamic Models

As was explained in the load modeling chapter, dynamic load models, and dynamic models in general are essential to capture the dynamic behavior of the system, especially with high motor loads and during transients. The following dynamic models are used for simulating the base case in time domain:

- Load composite model (cmpldw): this model was assigned to the load buses close to the most severe contingency (12 buses). It also contains the parameters for the different types of motors it represents.

- Synchronous generator (gencls): it represents the classical generator model (8 generators).
- Solid rotor generator (genrou): represented by equal mutual inductance rotor modeling (9 generators).
- Excitation system (exac1): IEEE type AC1 excitation system (9 generators).
- Over-excitation limiter (oel1): over-excitation limiter for synchronous machines excitation systems (9 generators). These models were added after it was noticed that some generators exceeded their reactive power capabilities following a large disturbance.
- Static VAr device (svcwsc): SVC model, compatible with WSCC standards (12 SVCs).
- Bus voltage recorder (vmeta).

4.5 Trajectory Sensitivity Index

Trajectory sensitivity index method has been used to investigate the voltage stability of the power system. Trajectory sensitivity index has also been found to be useful in finding the proper location for fast dynamic reactive power support [16]. In this work, trajectory sensitivities are used as weights in the objective function of the optimization problem since they describe the voltage response of load buses when reactive power is injected at a transmission or sub-transmission level bus. The trajectory sensitivity index (TSI) can be evaluated using the following formula:

$$TSI_j = \sum_{k=1}^{N_k} W_k \left[\sum_{i=1}^{n} W_{bi} \left[\frac{\partial |V_i|}{\partial Q_j} \right]_{t=t_k} \right] \tag{4.1}$$

where,

j: transmission or sub-transmission bus number where the reactive power is injected.

i: low voltage bus (load bus) where the voltage response is of interest.

W_k: weighting factor to designate the importance of time instant k, $W_k \in \{0, 1\}$.

N_k: number of time instants.

W_{bi}: weighting factor to designate the importance of bus i, $W_{bi} \in \{0, 1\}$.

n: number of load buses.

V_i: RMS ac voltage on bus i.

Q_j: reactive power injected at bus j.

4.6 Linear Programming

Linear programming was the mathematical tool used to optimize the amount of reactive power needed in order to prevent voltage recovery delays as well as maintaining the load buses voltage within acceptable limits following a large disturbance close to the load centers. Dynamic simulation using PSLF-GE software was performed, and the amount of reactive power needed was optimized for each time step for total time duration of two seconds following the instant of clearing the fault. The general form for linear programming is as follows:

$$\min_x f^T x, \; such \; that \begin{cases} Ax \leq b, \\ A_{eq}x = b_{eq,} \\ lb \leq x \leq ub. \end{cases} \tag{4.2}$$

where,

f: is the objective (cost) function, presented as a vector.

x: the set of variables, presented as a vector.

lb and *ub*: are the lower and upper bounds allowed for the variables, presented as vectors.

A and A_{eq}: are the constraints inequality and equality matrices respectively.

The objective function to be minimized is the total injected reactive power with constraints on the voltage level and SVC size. The optimization approach is formulated as follows:

Let $S_j(t)$ represents the trajectory sensitivity of bus *j* at the time instant *t*;

$$S_j(t) = \sum_{i=1}^{n} W_{bi} \frac{\partial |V_i(t)|}{\partial Q_j} \tag{4.3}$$

The trajectory sensitivities are used as weights in the objective function as follows:

$$\min_{Q_j} \sum_{j=1}^{N_j} S_j(t) Q_j \tag{4.4}$$

And the constraints are,

$$V_i^{min} \leq \left|V_i^0(t)\right| + \sum_{j=1}^{N_j} \frac{\partial |V_i(t)|}{\partial Q_j} Q_j \leq V_i^{max} \tag{4.5}$$

$$Q_j^{min} \leq Q_j \leq Q_j^{max} \tag{4.6}$$

where,

V_i^{min}, V_i^{max} are the acceptable predefined minimum and maximum RMS voltage levels at load bus *i*, respectively, at all time instants.

$V_i^0(t)$: is the uncompensated RMS voltage level at load bus i at instant t (without VAr injection)

Q_j^{min}, Q_j^{max}: are the allowed minimum and maximum amounts of VAr injection, respectively.

The trajectory sensitivity $S_j(t)$ is calculated by injecting 1 p.u. of reactive power at bus *j*, and for each *j* summing up the voltage level changes at load buses for all i, for each time step.

It should be noted here that the voltage level constraint in equation (4.5) is considered as a conservative constraint since it assumes that simultaneous VAr injections at different buses will result in voltage increments that are all in phase with each other. However, study results presented in Chapter 5 show that the voltage levels increased in each time step when optimal VArs are injected at optimal locations. This proves that the approximation introduced by this inequality is minimal, and that the phase shift between voltage increments is not significant since voltages add up for each time step, resulting in a higher overall voltage magnitude.

For time steps following the fault clearance instant, voltage magnitude will still be very low (depending on the disturbance severity) even with VAr injection since voltage at load buses cannot be recovered to its normal values instantaneously. Therefore, it is more realistic to have a changing value for V_i^{min} that would be increased gradually in each time step. In this work V_i^{min} was cho-

sen to be directly related to $V_i^0(t)$ for each time step, which makes V_i^{min} time dependant as well. In this work the minimum allowed voltage level for each time step is defined as follows:

$$\left|V_i^{min}(t)\right| = 1.15\left|V_i^0(t)\right| \tag{4.7}$$

Therefore, at each time step the optimization function will calculate the least required amount of VAr injection needed to increase the voltage level by 15% above its uncompensated value for each load bus. The value of 15% increase was chosen for the following reasons:

- It provides a realistic recovery rate for voltage levels at load buses.
- It provides acceptable voltage levels for the last time step in the optimization process; after two seconds of clearing the fault, the lowest voltage level is around 0.7 p.u.
- It minimizes the number of unsolved (infeasible) cases in the optimization process.

It should be noted here that $V_i^{min}(t)$ is assigned a maximum value (i.e. 0.95 p.u.) to ensure that it is always kept below V_i^{max}. V_i^{max} is considered to be 1.05 p.u. although it does not affect the optimization results since it is a minimization problem.

4.7 Generalizing Results

Since the optimization process is performed for each time step, the outcome of this procedure is a set of optimized values of Q_j for each time step as well. Each set contains the values of VAr injection needed by each SVC. In order to achieve one set of VAr injection optimal values that represents all the sets at

different time steps, an averaging procedure is required. However, in the averaging process higher weights should be assigned to the more critical time steps. Critical time steps here refer to the time steps following the fault clearing instant when the voltage levels are at their lowest point. VAr compensation is needed the most at these critical time steps to prevent voltage recovery delays caused by motors stalling. The optimized objective function value will be relatively low at these critical time steps because $V_i^{min}(t)$ is at its lowest levels. Therefore, a weighting factor that is inversely proportional to the objective function value is used for each time step. This will ensure that the VAr compensation needs for these critical time steps will have better representation in the overall average for all time steps. The weighted sets are then averaged over all the time steps to evaluate the final optimal VAr injection values. The averaging procedure can be presented as follows:

$$Q_T = \frac{\sum_{k=1}^{N_k} \left[\frac{Q_j}{f(Q_j)}\right]_{t=t_k}}{N_k} \tag{4.8}$$

where,

Q_T: is the total weighted and averaged set of VAr injection values.

$f(Q_j)$: is the value of the objective function at a given time instant.

This new total set of VAr injection values represents a single operating condition and contingency case, while the objective of this work is to find a set of VAr compensation values that is valid for different operating conditions and contingencies. Therefore, the load at the buses that are being investigated (i buses) was increased in order to change the operating conditions by representing load growth.

The load was increased by 5%, 15% and 20%. For each new operating condition, the voltage sensitivities were recalculated, and the optimization and averaging procedures were performed again. Consequently, four sets of the total weighted and averaged VAr injection values were generated; one for the base case (no load increase), and three for the increased load cases. In order to compose a final set of VAr compensation values that represents the different operating conditions, the highest value of VAr compensation was chosen from each case set for every bus. Therefore, in the final optimized set of VAr compensation values, each SVC was assigned its highest value in the different operating conditions. For different contingencies, there is no need to run the whole process again since the base contingency chosen is considered to be the most severe. Therefore, different contingencies were used to validate the final set of VAr compensation values (SVC sizes).

CHAPTER 5

STUDY RESULTS

5.1 System Representation

An IEEE, 162-bus, 17-generator test case [26] is used throughout this work. This test case consists of one area and twelve zones. Table 5.1 shows the overall system components. The total generation is 15,546 MW, while the total load is 15,387 MW.

Table 5.1 System components

Component	Number
Buses	162
Generators	17
Shunts	34
Lines	238
Transformers	46
Load Aggregations	89

5.2 Base Contingency Selection

In order to select the most severe credible contingency, several three-phase faults were applied at several 345 kV buses located near major load centers, and the voltage dips at the 69 kV load buses were monitored. These faults were cleared after 6 cycles by opening a 345 kV line. The criteria for selecting the most severe contingency are the magnitude of voltage dips at load buses, and the number of affected buses by that contingency. Therefore, a contingency is considered

severe if it causes a significant voltage dips on a large number of load buses. Worst Condition Analysis (WCA) feature in PSLF-GE was used to scan voltage dips all over the system buses following a contingency. WCA scans for buses whose voltage level change exceeds a predefined value for a certain amount of time. In order to find the most severe contingency, a change percent in voltage level of 50% for 0.1 seconds was chosen as the threshold for WCA. Therefore, any bus whose voltage level dips below 50% of its initial level for 0.1 seconds or more is recorded. This threshold is chosen since a 50% (or more) dip in voltage level for at least 0.1 seconds at a load bus will very likely cause most of the running motors to stall. After running WCA for several contingencies, it was found that a three-phase fault on bus 120 "S3456 3" would cause 12 load buses to violate the limit predefined in WCA. Table 5.2 shows the representative numbers, voltage level and load. Figures 5.1-5.2 show the load buses affected by the most severe contingency. It should be noted that these loads are represented by static models and are located at the transmission voltage level. Voltage magnitude plots have been divided into two graphs (sets) throughout this chapter for clarity purposes.

Table 5.2 Representative load buses

Bus number	Voltage kV	Load MW
111	161	65.41
133	69	30.1
134	161	17.46
135	69	20.06
136	69	20.06
137	69	20.06
139	69	10.1
140	69	13.58
143	69	21.07
144	69	12.37
145	69	10.83
146	69	21.33

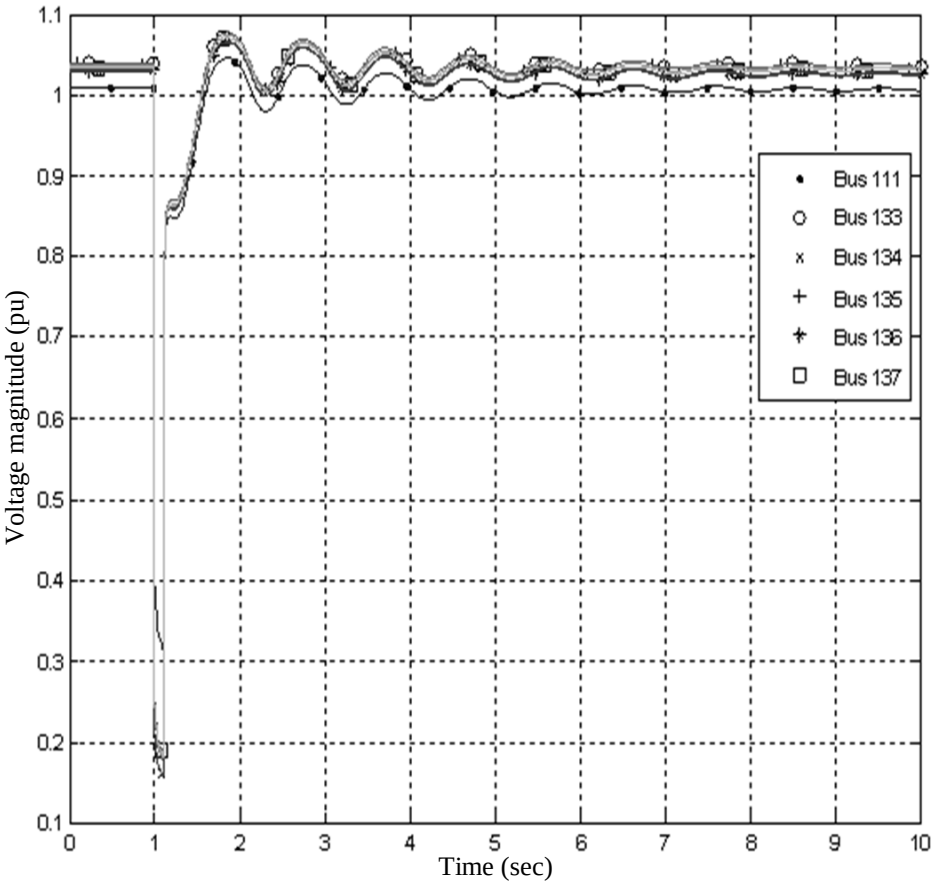

Figure 5.1 Load bus voltage magnitude (static load models) set-1

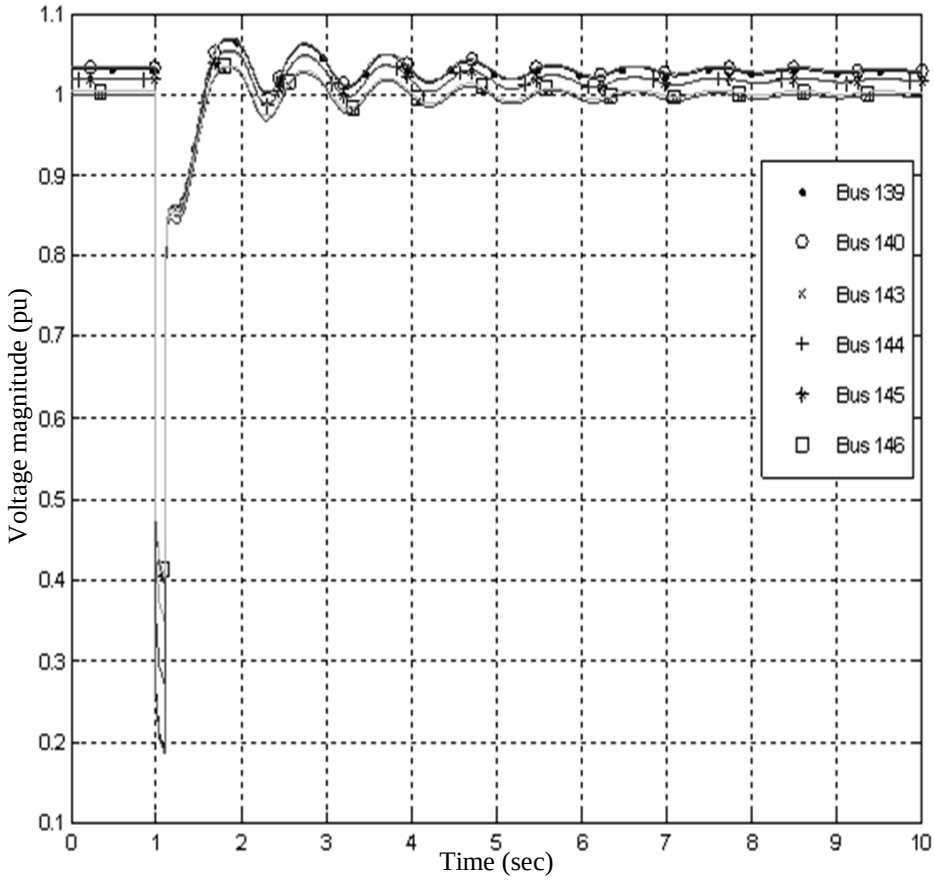

Figure 5.2 Load bus voltage magnitude (static load models) set-2

5.3 Dynamic Load Modeling

The power flow model for the test case used in this work represents the system down to the sub-transmission level, and the loads are aggregated and connected to the transmission or sub-transmission levels. Therefore, the load buses represented in Figures 5.1-5.2 are either rated at 161 kV or 69 kV. In order to represent the loads affected by the base contingency more realistically and accurately, those 12 load buses were stepped down through distribution transformers to the 12.47 kV level, and the new low voltage buses were assigned the numbers 163-174. It is also necessary to include motor models within the representative load buses in order to capture the dynamic behavior of these loads. The impor-

tance of dynamic models can be concluded from Figures 5.1-5.2; which show that the voltage magnitude for those load buses recovered almost instantaneously despite of the large disturbance which caused a significant voltage dip. The voltage recovered to its normal value very fast because the dynamic behavior of motors, such as: decelerating and stalling, is not represented in the static load models.

The composite load model provided by PSLF-GE (cmpldw) was used to include motor models along with the static part of the load. The composite load model (cmpldw) complies with the composite load model developed by WECC LMTF shown in Figure 2.5. [27] cmpldw includes the models of the following:

- Distribution network: This includes the substation components, such as: transformers, shunts and feeders. However, this part was not included in this work because the loads were already stepped down to the distribution level.
- Static loads: Part of the load was represented by static models. The real power part of the static loads was represented as constant current, while the reactive power part was represented as constant impedance.
- Motors: it is possible to represent up to four different motor types in cmpldw. It is also possible to represent both, three-phase induction motors as well as single-phase motors. In this work 72% of the total load is assumed to be motors [1]. 10% of the motors are modeled as large industrial motors (high inertia), while

around 50% of the motors are modeled as single-phase A/C motors, and the rest as small induction motors.

Figures 5.3-5.4 show the voltage magnitude for the representative load buses after applying the base contingency. In these figures the loads were located at the low voltage side of the network and represented by the composite dynamic load model.

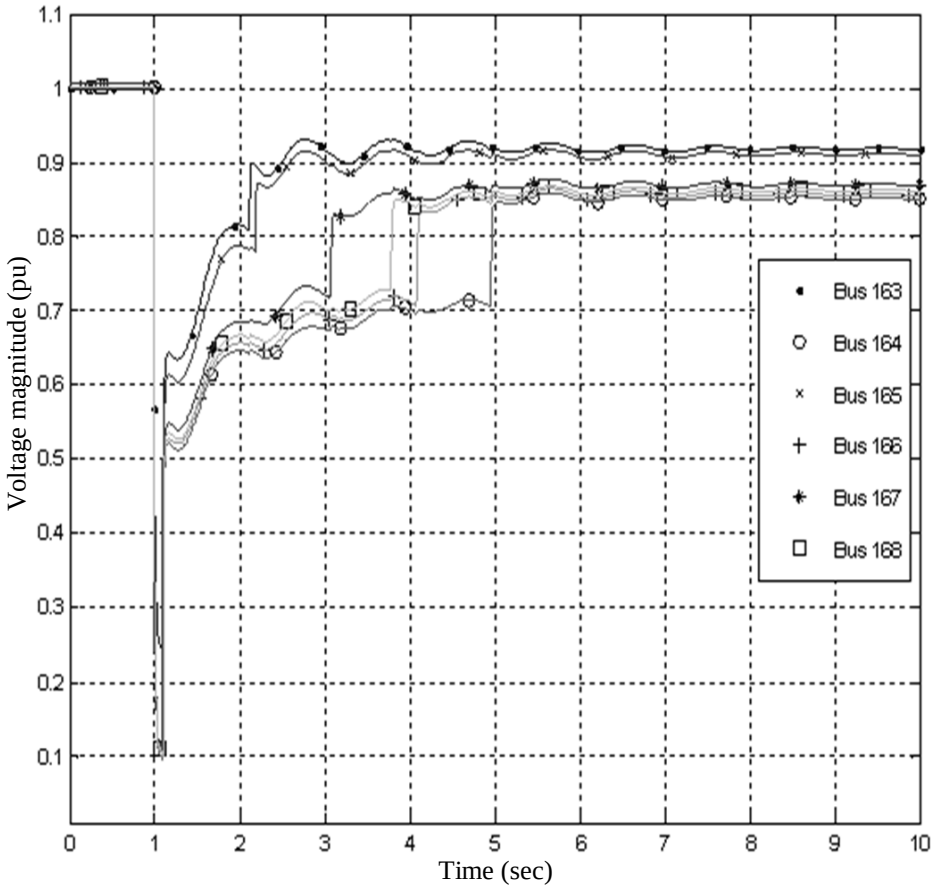

Figure 5.3 Load bus voltage magnitude (dynamic load models) set-1

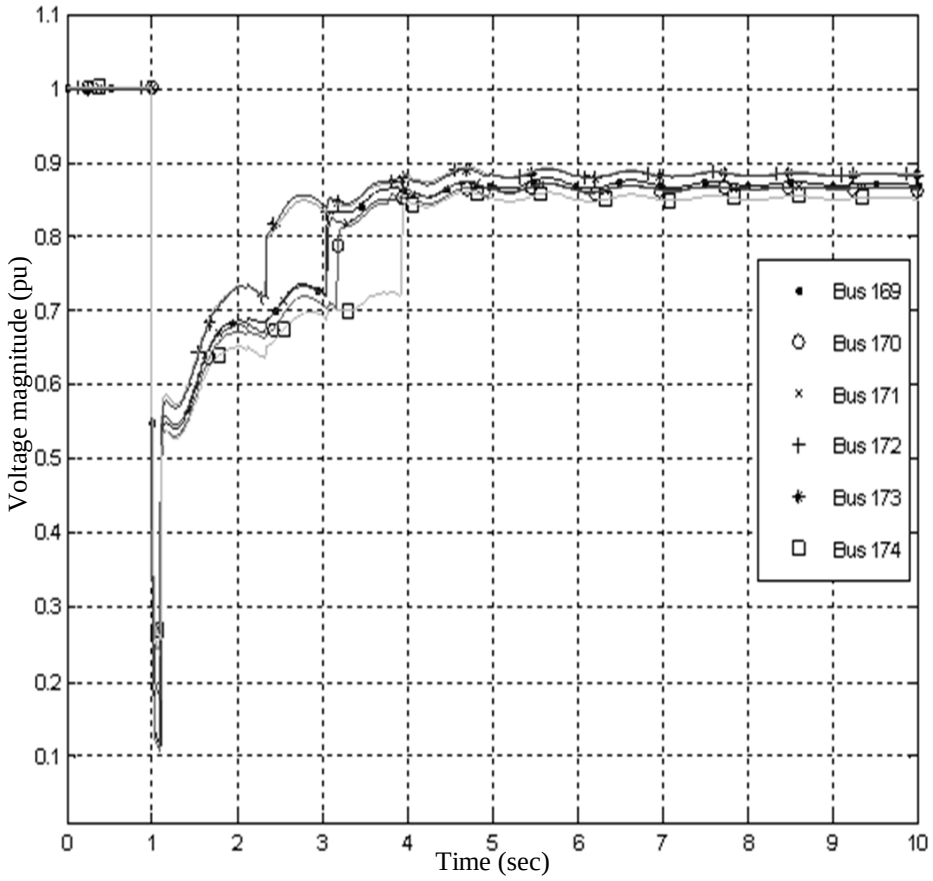

Figure 5.4 Load bus voltage magnitude (dynamic load models) set-2

Figures 5.3-5.4 show that when representing the dynamic models of motors the voltage recovery is delayed because of the deficiency in reactive power caused by stalled motors. Figures 5.3-5.4 also show that some buses needed up to 4 seconds to partially recover after clearing the fault, while Figures 5.2-5.3 show a full voltage recovery after less than 0.5 seconds after clearing the fault.

The voltage magnitudes in Figures 5.3-5.4 recovered to a value close to its initial level because part of the stalled motors (60%) were allowed to reaccelerate if their voltage magnitude increases to 0.7 p.u. Therefore, each time the stalled motors at a certain load bus start to reaccelerate, the voltage magnitude will increase and will cause other stalled motors on different buses to reaccelerate.

However, since a portion of the stalled motors does not reaccelerate, the voltage magnitude will not recover to its initial level. The remaining stalled motors have to be tripped by thermal protection in order to achieve a full voltage recovery. Thermal protection is not modeled in this work because the time constant for thermal relays is very large compared to the time frame of short term voltage stability.

5.4 Trajectory Voltage Sensitivity Results (base case)

Trajectory voltage sensitivities are used in this work as weighting factors in the optimization problem since they describe the voltage magnitude response with respect to reactive power injection. Therefore, dynamic time domain analysis is used to determine the voltage sensitivities of the high voltage buses which are considered for SVC placement.

In order to obtain a comprehensive solution and to test the optimization process over several buses with different sensitivities, all the high voltage buses in Table 5.2 which are directly connected to the representative low voltage load buses are considered as VAr injection candidate buses in the optimization process. Therefore, for each bus in Table 5.2 the trajectory voltage sensitivity $S_j(t)$ was evaluated for each time step as shown in equation (4.3). At fault clearing time instant a 1 p.u. of fixed VAr injection was applied at each bus sequentially, and for each bus the voltage change at the low voltage load buses was recorded. Table 5.3 shows the trajectory sensitivity indices (TSI_j) for the VAr injection buses.

Table 5.3 TSIj for VAr injection buses

Bus number j	TSI_j
111	39.23
133	79.80
134	41.37
135	90.43
136	92.73
137	94.53
139	87.54
140	94.70
143	136.73
144	105.43
145	114.09
146	140.84

5.5 Optimization Results (base case)

A simple Matlab code is used to evaluate the linear programming problem described by the equations (4.4), (4.5) and (4.6). The Matlab code uses the following inputs:

- Trajectory voltage sensitivities $S_j(t)$ for each time step.
- The uncompensated voltage level at load bus i, $(V_i^0(t))$ for each time step.

- The allowed minimum and maximum size of SVC, Q_j^{min}, Q_j^{max}. In this work the bounds for SVC size in p.u. are: $Q_j^{min} = 0$, $Q_j^{max} = 2$.

The outputs of this code are:

- A set of optimal VAr injection values Q_j for each time step.
- The value of the optimal objective function for each time step.

5.5.1 Non-weighted Results

Table 5.4 shows the non-weighted, averaged values of the optimal VAr injection evaluated by the optimization process.

Table 5.4 Optimized, non-weighted VAr injection values (base case)

Bus number j	Q_j p.u.
111	0.652
133	1.506
134	1.547
135	0.789
136	0.000
137	0.082
139	0.012
140	0.002
143	0.030
144	0.259
145	0.036
146	0.041
Total	4.956

As shown in Table 5.4, some buses were assigned very low (negligible) VAr injection values if any, such as: buses 136, 140 and 139. Therefore, the optimization process not only determines the optimal amount of VAr injection, but also determines the optimal locations for VAr injection. Figures 5.5-5.6 show the voltage response at low voltage load buses while VArs are injected according to Table 5.4.

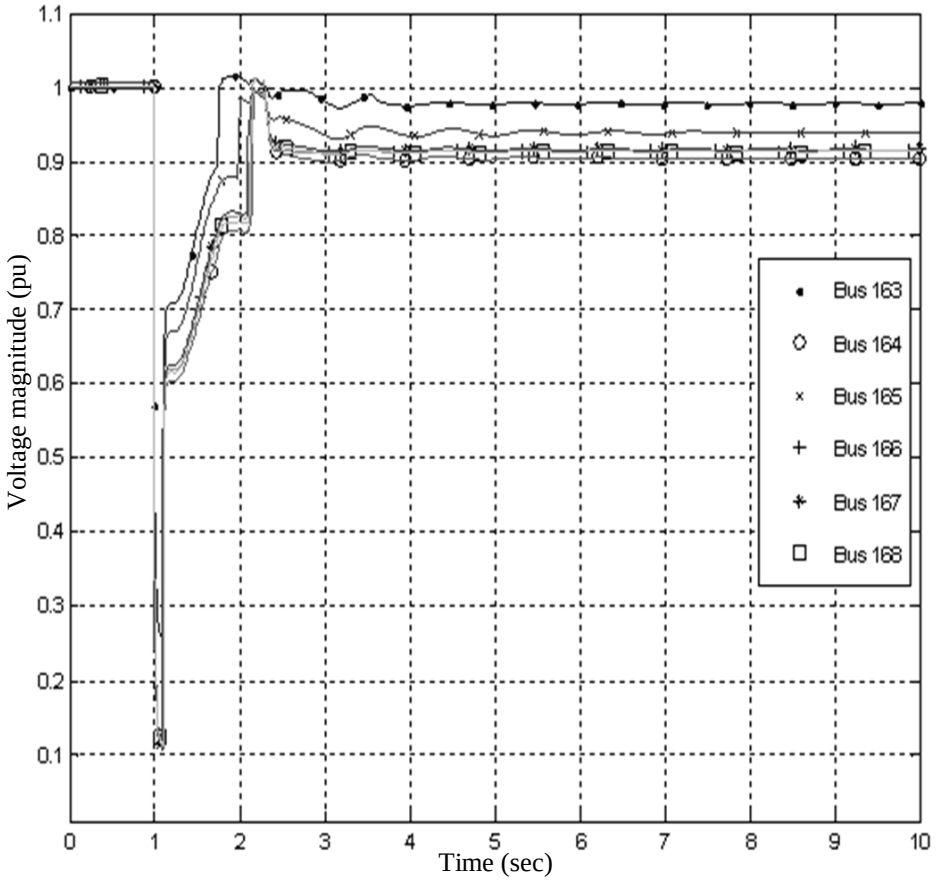

Figure 5.5 Load bus voltage magnitude with VAr injection (non-weighted) set-1

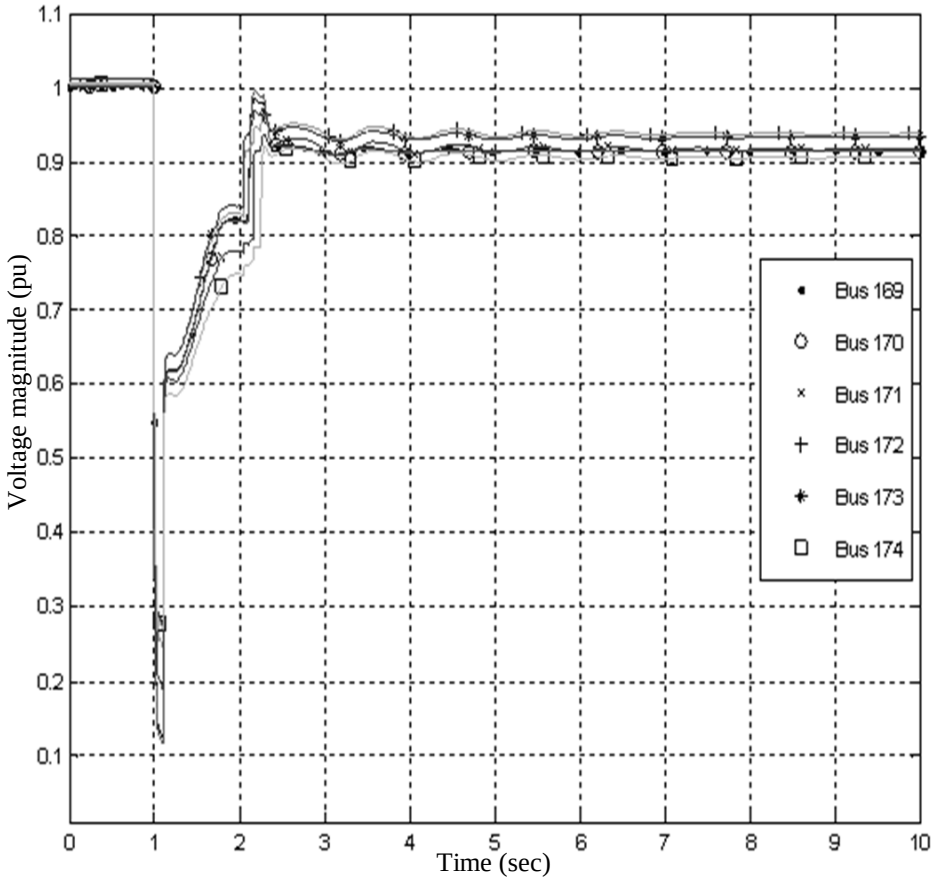

Figure 5.6 Load bus voltage magnitude with VAr injection (non-weighted) set-2

Compared to Figures 5.3-5.4, the voltage recovery shown in Figures 5.5-5.6 with optimal VAr injection is much faster, one second after fault clearing the voltage magnitudes at all buses were above 0.9 p.u., also the final voltage magnitude is higher when VArs are injected.

5.5.2 Weighted Results

In order to assign weights for each set of optimal VAr injection values for each time step, the objective function value is used as shown in equation (4.8). Table 5.5 shows the weighted, averaged values of the optimal VAr injection evaluated by the optimization process.

Table 5.5 Optimized, weighted VAr injection values (base case)

Bus number *j*	*Qj* p.u.
111	0.455
133	1.034
134	1.066
135	0.523
136	0.000
137	0.057
139	0.009
140	0.002
143	0.022
144	0.174
145	0.024
146	0.029
Total	3.396

Figures 5.7-5.8 shows the voltage response at low voltage load buses while VArs are injected according to Table 5.5.

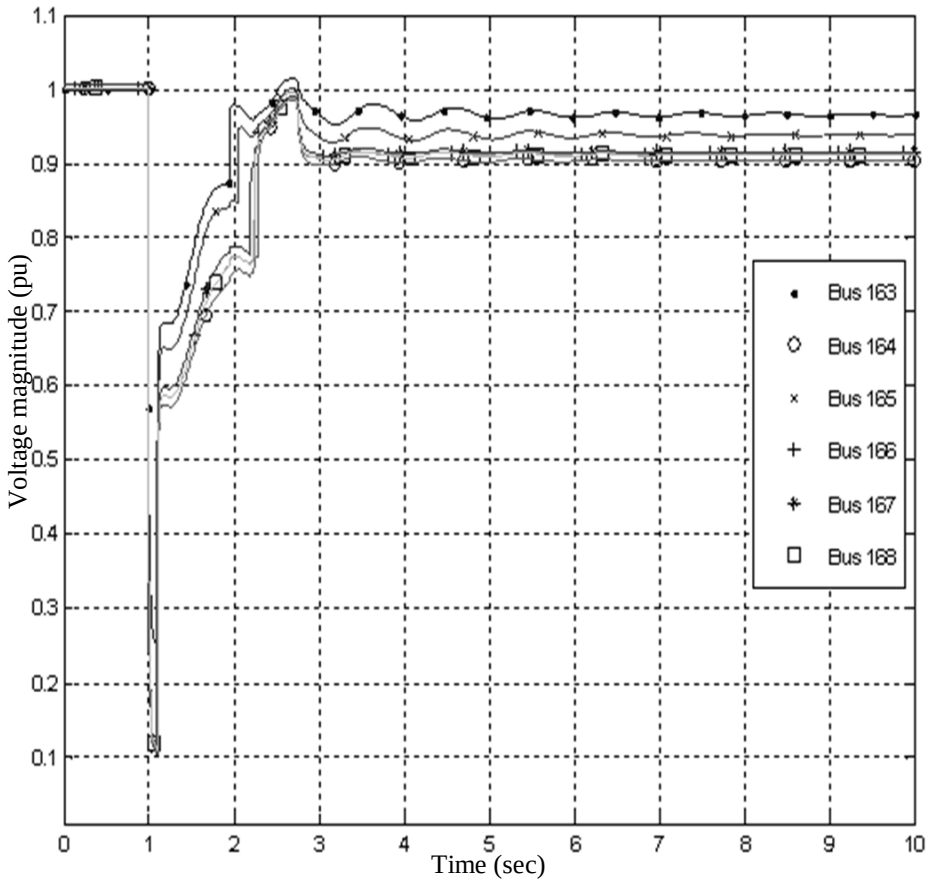

Figure 5.7 Load bus voltage magnitude with VAr injection (weighted) set-1

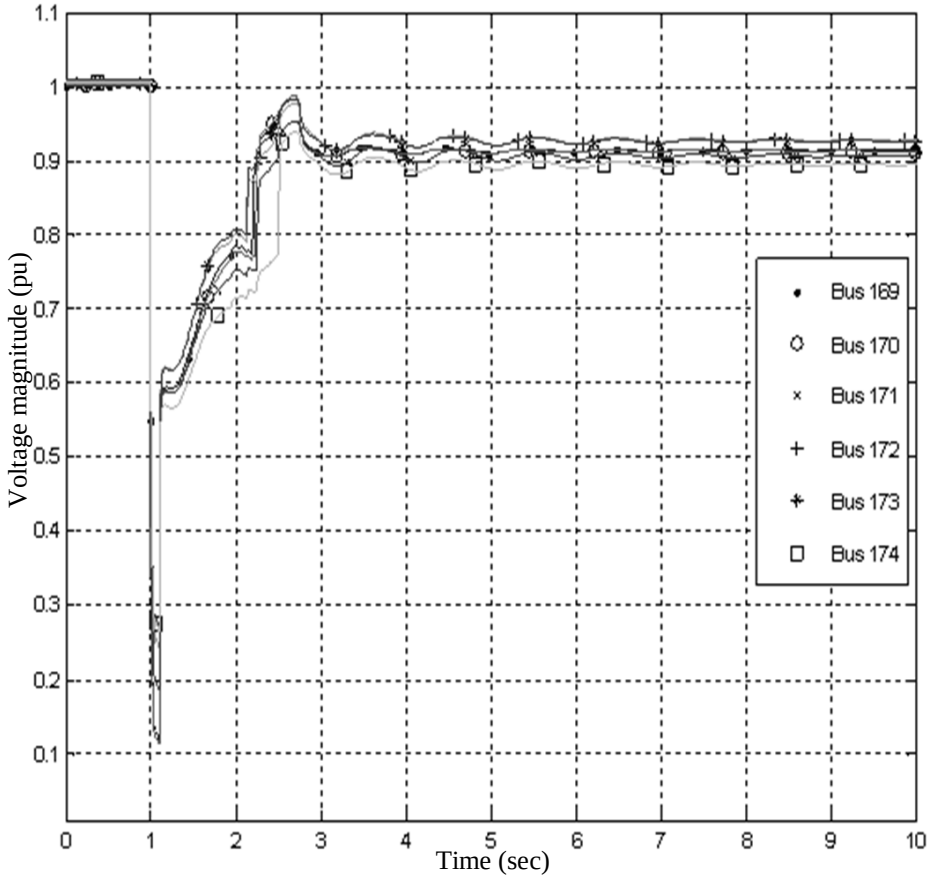

Figure 5.8 Load bus voltage magnitude with VAr injection (weighted) set-2

As shown in Figures 5.7-5.8, voltage recovery in the weighted case was almost as fast as it is in the non-weighted case although the total of weighted VAr injection is more than 30% less than the non-weighted case. This proves the importance of giving higher weights to the critical time steps when the voltage magnitude is very low than the following time steps with relatively high voltage magnitude.

5.6 The Relation Between Voltage Trajectory Sensitivity and Optimal VAr Injection

Table 5.6 shows the trajectory sensitivity indices (TSI_i) for each VAr injection bus and its corresponding optimal value of VAr injection.

Table 5.6 Bus trajectory sensitivity indices and corresponding optimal VAr injection

Bus number *j*	*TSIj*	*Qj* p.u.
111	39.23	0.455
133	79.80	1.034
134	41.37	1.066
135	90.43	0.523
136	92.73	0.000
137	94.53	0.057
139	87.54	0.009
140	94.70	0.002
143	136.73	0.022
144	105.43	0.174
145	114.09	0.024
146	140.84	0.029

Table 5.6 shows that the optimization process has assigned very low values of VAr injection to buses with high sensitivity such as: 146, 143 and 145, compared to less sensitive buses such as: 111, 133 and 134. This correspondence can be explained by examining the nature of the SVC operation. Controls in SVC increase the effective admittance when the voltage level drops below a certain value, and if more VAr injection is needed the effective admittance will be increased more till the SVC is represented as a shunt capacitor. However, whenever the voltage level starts to recover the SVC effective admittance will be decreased

accordingly to ensure the voltage level stays within an acceptable range. Therefore, if a large SVC was located at a very sensitive bus, the voltage level of that bus will need a small amount of VAr injection and will recover very fast, which will cause the effective admittance of the SVC to drop down to very low values in a short time. However, if a large SVC was located at a less sensitive bus, the voltage level on that bus will need more time to recover, therefore, the effective admittance of the SVC will be kept at high levels for longer time, which will cause more VArs to be injected into the system and therefore increase the voltage magnitudes of other load buses. To illustrate the SVC output with respect to the voltage sensitivity, Figure 5.9 shows the effective admittance (p.u.) for two separate cases where a 1 p.u. SVC is located on bus 137 (high sensitivity), and on bus 111 (low sensitivity).

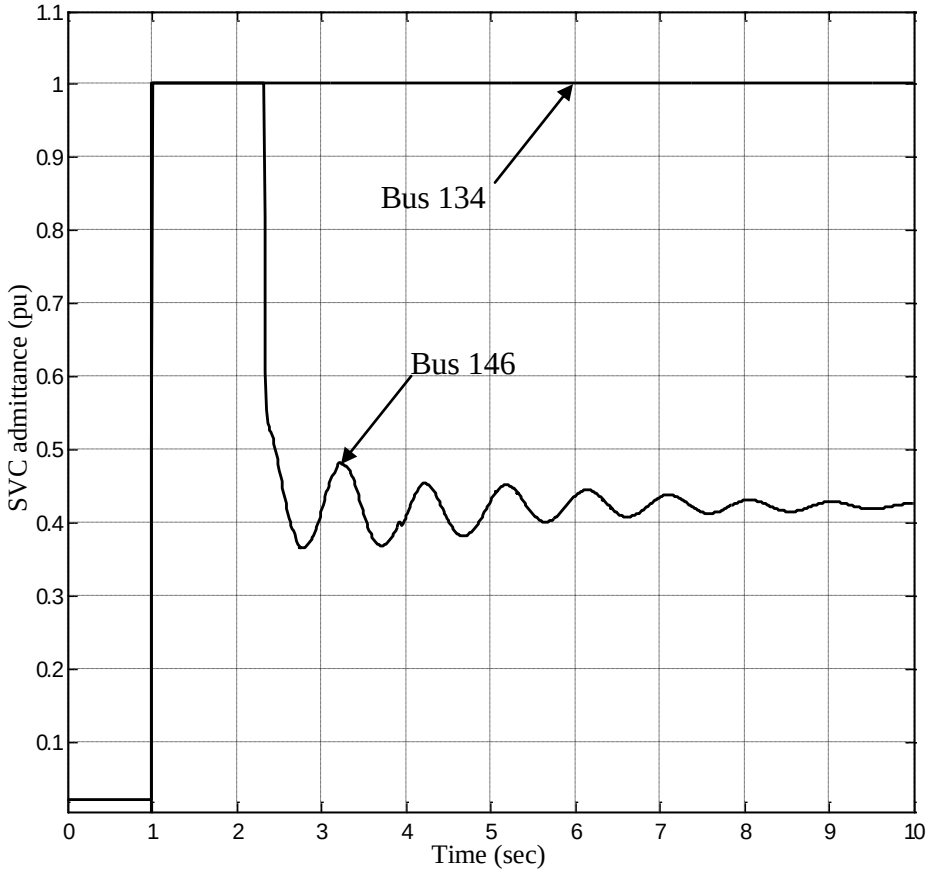

Figure 5.9 SVC effective admittance with respect to bus sensitivity

5.7 Different Operating Conditions Results

In order to evaluate an optimal set of VAr injection that is valid for different operating conditions, the load at the representative load buses was increased to examine the effect of load growth over the optimal amount of VAr injection needed. The load was increased by 5%, 10%, 15% and 20%, and for each case the optimal amount of VAr injection was evaluated. Table 5.7 shows the TSI_j for the VAr injection buses, for each different operating condition.

Table 5.7 Bus trajectory sensitivity indices for different operating conditions

Bus number *j*	TSI_j			
	Case-1 (5%)	Case-2 (10%)	Case-3 (15%)	Case-4 (20%)
111	31.52	38.56	26.82	26.11
133	53.56	52.47	37.37	35.16
134	28.11	30.21	22.92	22.18
135	56.22	54.83	39.27	36.75
136	76.05	80.00	56.08	44.25
137	78.29	59.34	43.88	40.93
139	74.27	78.24	55.07	43.26
140	78.82	63.73	44.53	41.39
143	116.54	119.57	109.58	100.46
144	92.02	91.07	81.97	68.77
145	90.12	89.77	81.08	77.44
146	125.19	130.88	122.92	111.06

Table 5.7 shows that in general the trajectory sensitivity indices decrease when the load is increased. However, when the load is increased it is expected that more VAr injection is needed. This can be concluded from Table 5.8 which shows the optimal weighted values of VAr injection for each different operating condition case.

Table 5.8 Optimized weighted VAr injection values for different operating conditions

Bus number *j*	*Qj* p.u.			
	Case-1 (5%)	Case-2 (10%)	Case-3 (15%)	Case-4 (20%)
111	0.502	0.591	0.546	0.584
133	1.079	1.303	1.484	1.486
134	1.280	1.243	1.411	1.506
135	0.694	0.714	0.743	0.821
136	0.000	0.034	0.000	0.000
137	0.072	0.085	0.098	0.114
139	0.021	0.026	0.029	0.060
140	0.017	0.016	0.023	0.054
143	0.033	0.038	0.043	0.059
144	0.194	0.115	0.161	0.153
145	0.030	0.008	0.009	0.010
146	0.035	0.050	0.056	0.061
Total	3.957	4.222	4.605	4.908

In order to compose a final set of VAr injection values that will be valid for all different operating conditions, the highest value of Q_j for each different operating condition is selected as the choice of the SVC rating for each bus. Table 5.9 shows the VAr injection values for the optimal final set.

Table 5.9 Final optimized VAr injection values

Bus number *j*	*Qj* p.u.
111	0.591
133	1.486
134	1.506
135	0.821
136	0.034
137	0.114
139	0.060
140	0.054
143	0.059
144	0.194
145	0.030
146	0.061
Total	5.011

Figures 5.10-5.11 show the voltage response at low voltage load buses for case-4 (20% increase in load) without any VAr injection present.

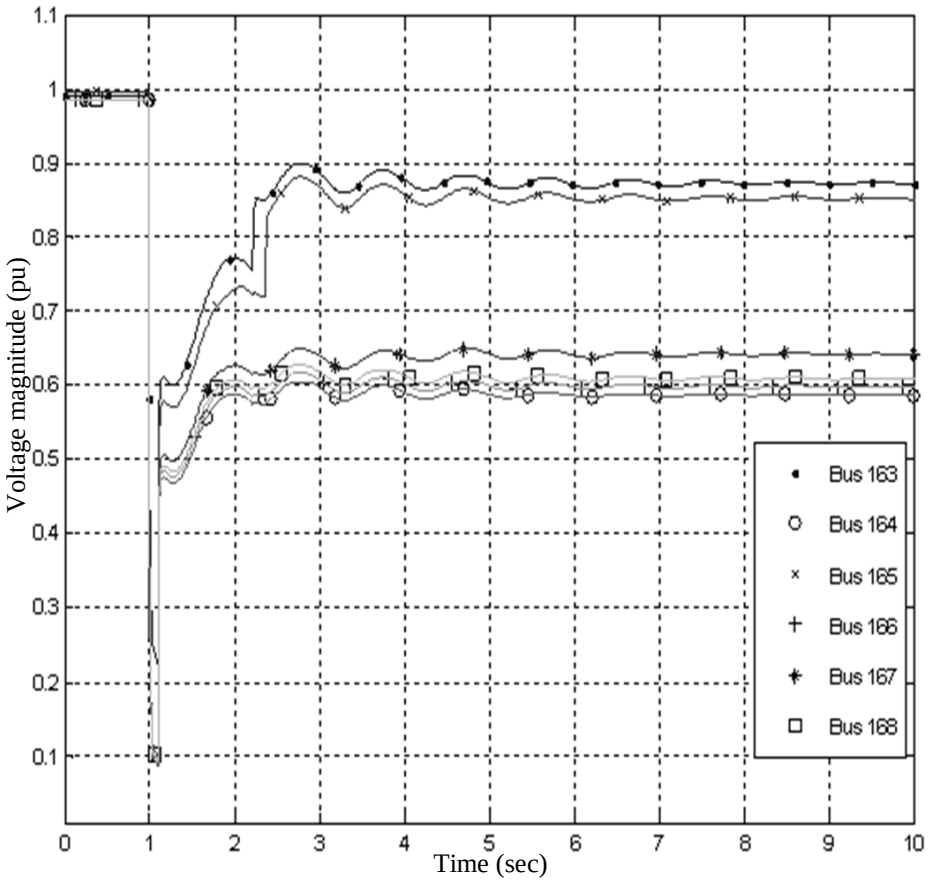

Figure 5.10 Load bus voltage magnitude without VAr injection (case-4) set-1

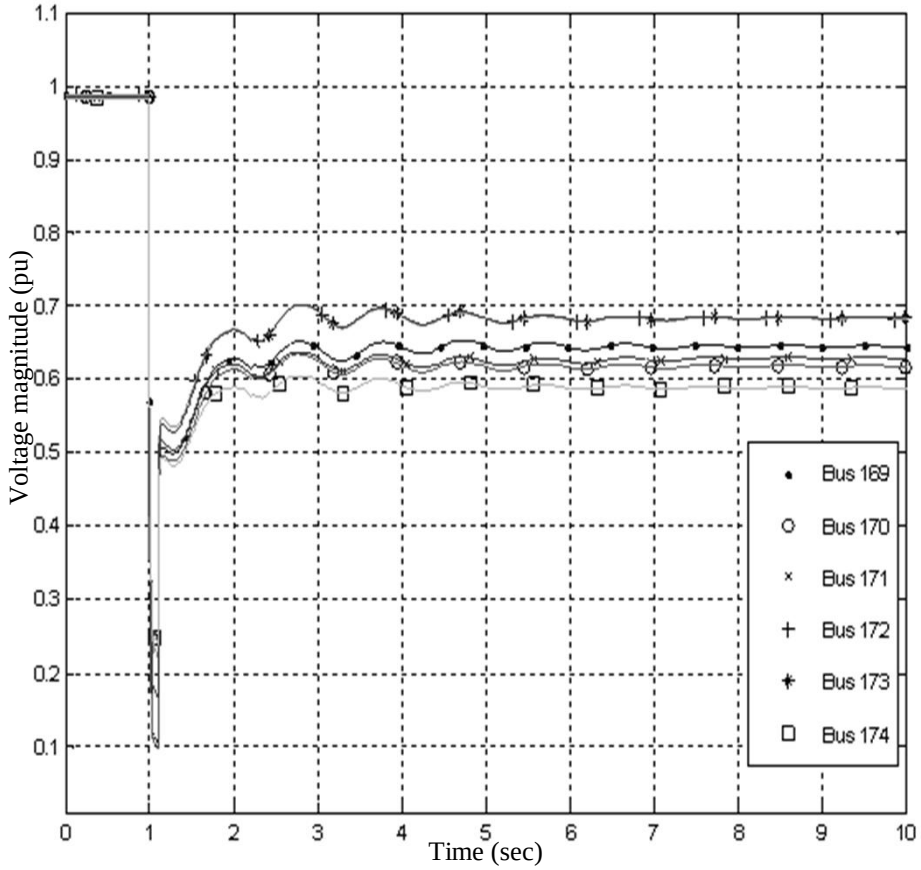

Figure 5.11 Load bus voltage magnitude without VAr injection (case-4) set-2

Figures 5.10-5.11 show that most of the load buses do not recover, and their voltage magnitudes stay depressed at very low levels because of the stalled motors. Such a scenario may cause a wide voltage collapse if these loads were not tripped. Figures 5.12-5.13 show the same case when VArs are injected according to Table 5.9. Figures 5.12-5.13 show that around 2 seconds after clearing the fault the voltage level of all the load buses recovered to acceptable values.

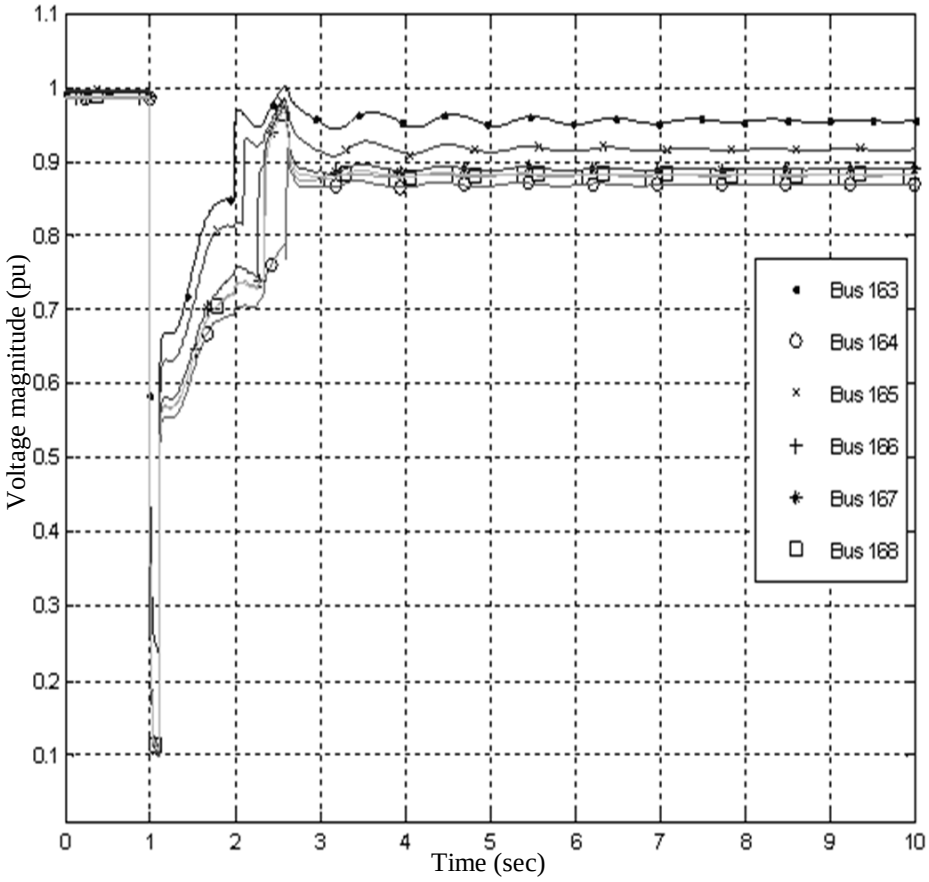

Figure 5.12 Load bus voltage magnitude with final VAr injection values

(case-4) set-1

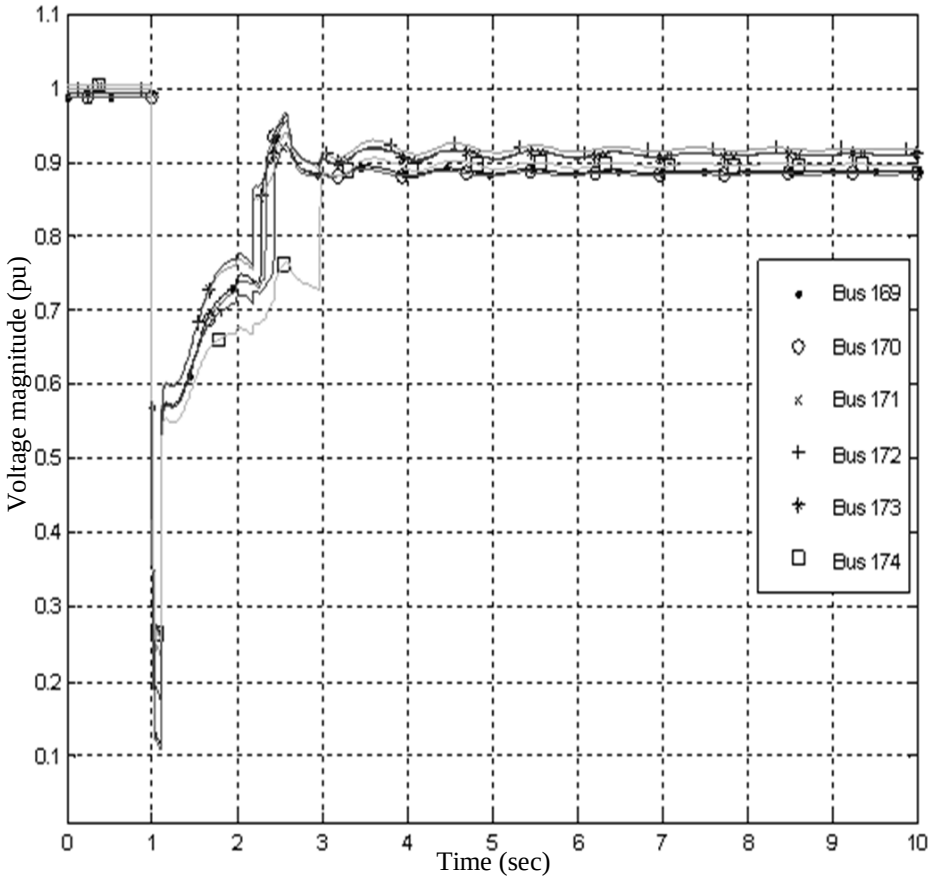

Figure 5.13 Load bus voltage magnitude with final VAr injection values

(case-4) set-2

5.8 A Description of Contingency Results

The optimized final set of VAr injection values should be capable of improving the voltage profile at load buses for a different number of contingencies. However, since this work used the most severe contingency to evaluate the optimized VAr injection values, the same values were used for the new contingencies. Therefore, another three 345 kV buses were chosen for the new contingencies; bus 5, 112 and 128. Figures 5.14-5.15 show the voltage response at low voltage load buses for contengincy-1 (fault at bus 5), and with 20% load increase, with final VAr injection set applied.

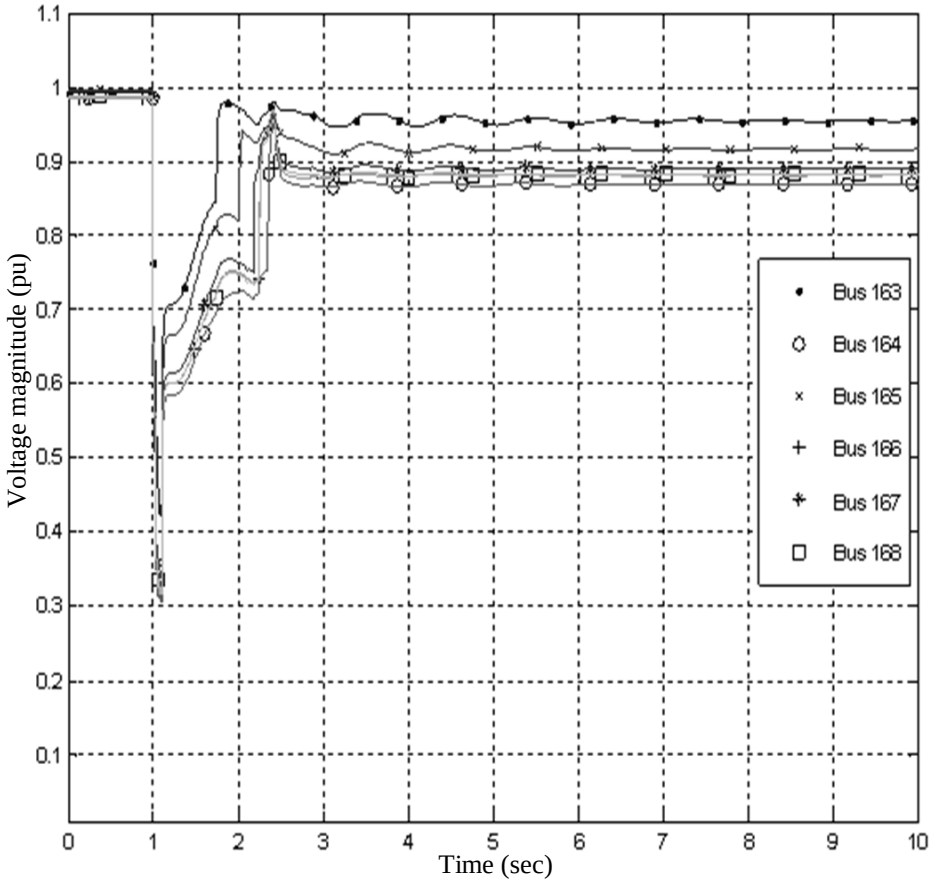

Figure 5.14 Load bus voltage magnitude with final VAr injection values

(fault at bus 5) set-1

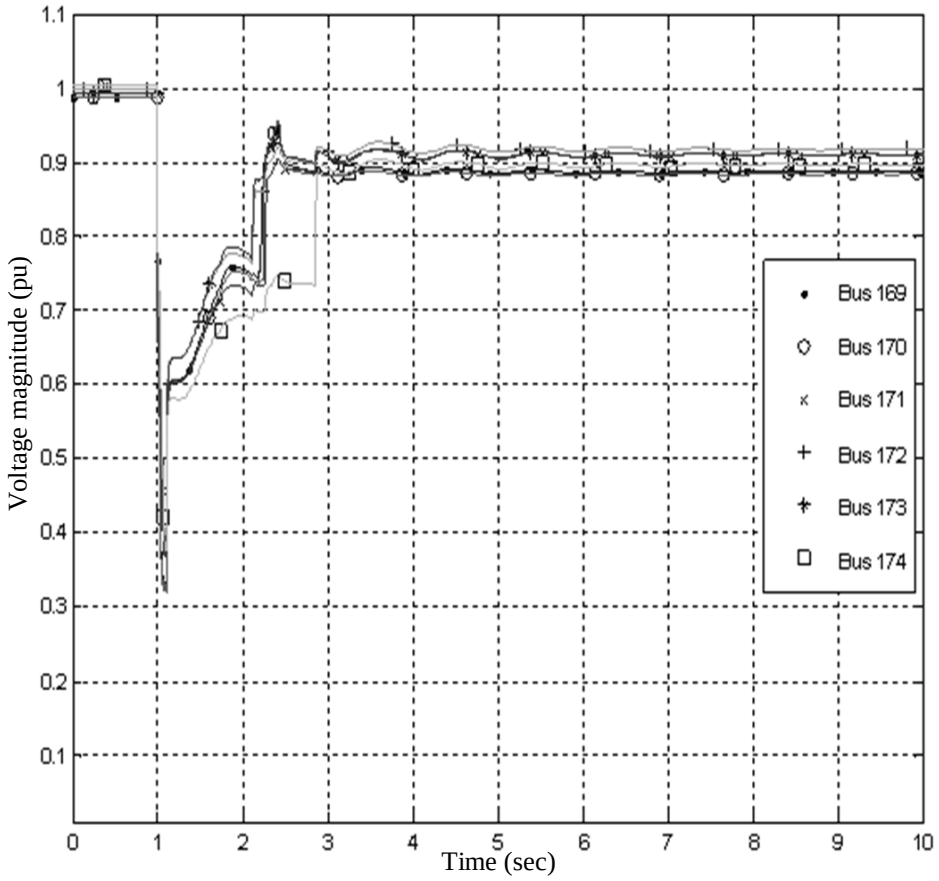

Figure 5.15 Load bus voltage magnitude with final VAr injection values (fault at bus 5) set-2

Figures 5.14-5.15 show that this contingency is less severe than the base case contingency since the voltage level dip during the fault is not as deep as the base case. The voltage recovery time also is less for this contingency. Figures 5.16-5.17 show the voltage response at low voltage load buses for contengincy-2 (fault at bus 112), and with 20% load increase, with final VAr injection set applied.

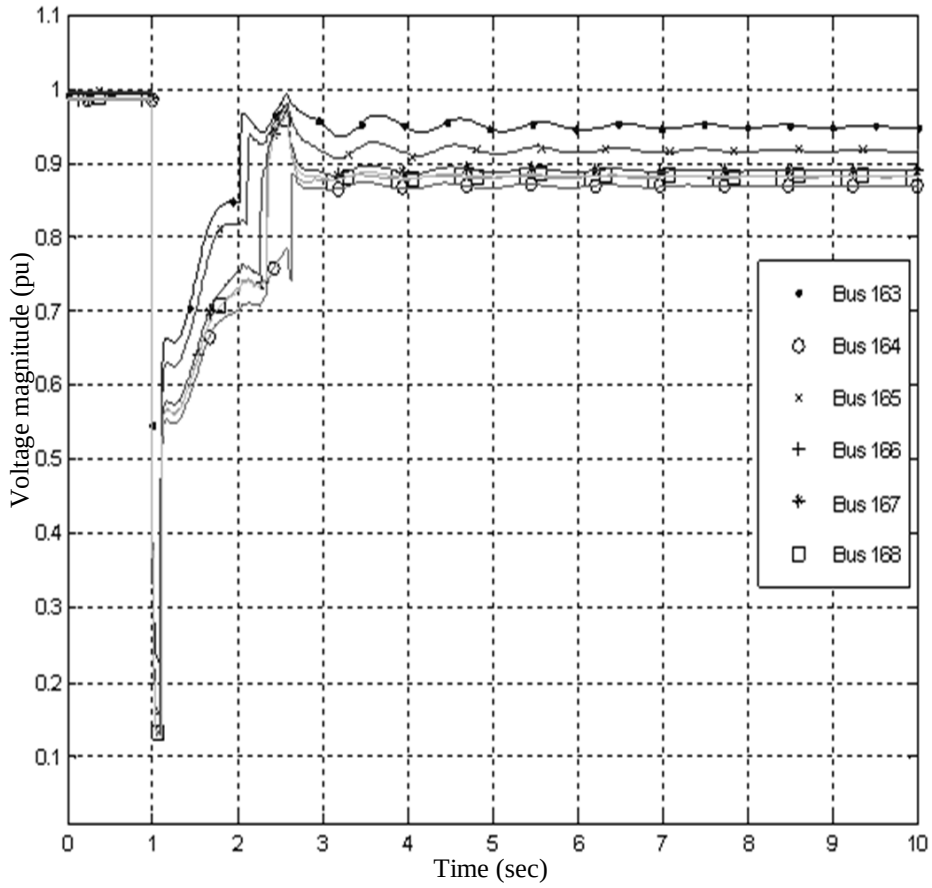

Figure 5.16 Load bus voltage magnitude with final VAr injection values

(fault at bus 112) set-1

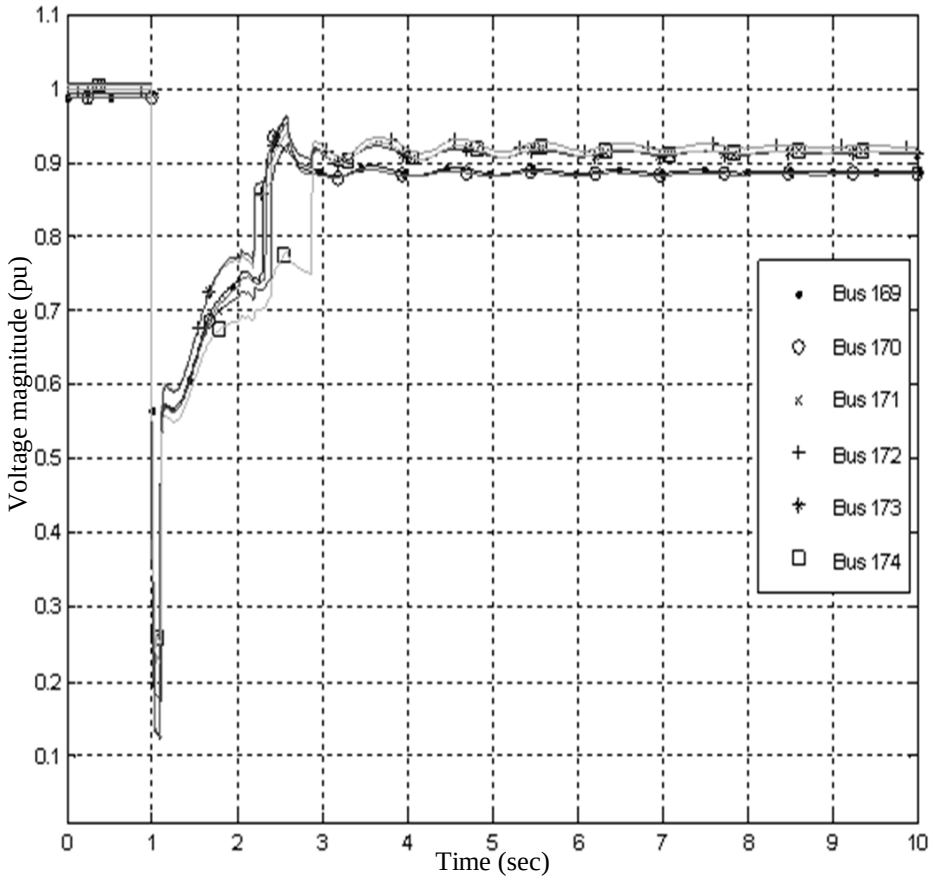

Figure 5.17 Load bus voltage magnitude with final VAr injection values (fault at bus 112) set-2

In Figures 5.16-5.17, although the voltage dips during the fault are as deep as it is in the base case, but the voltage recovery time is less for this contingency. Figures 5.18-5.19 show the voltage response at low voltage load buses for contengincy-2 (fault at bus 128), and with 20% load increase, with final VAr injection set applied.

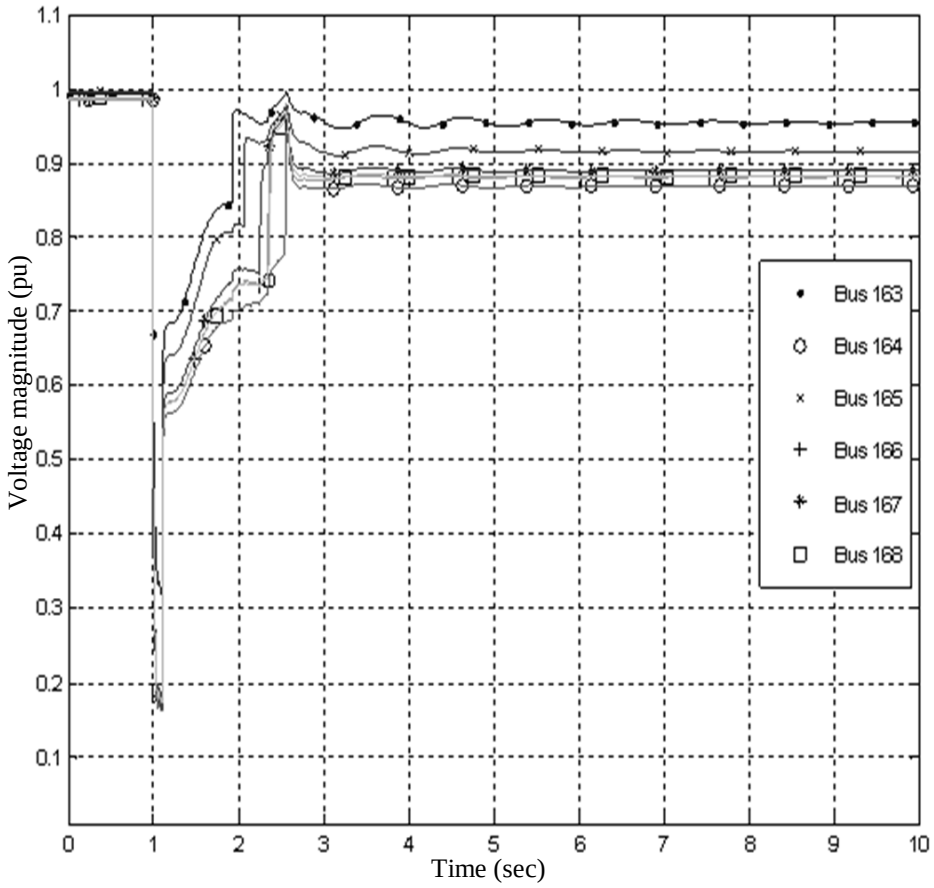

Figure 5.18 Load bus voltage magnitude with final VAr injection values

(fault at bus 128) set-1

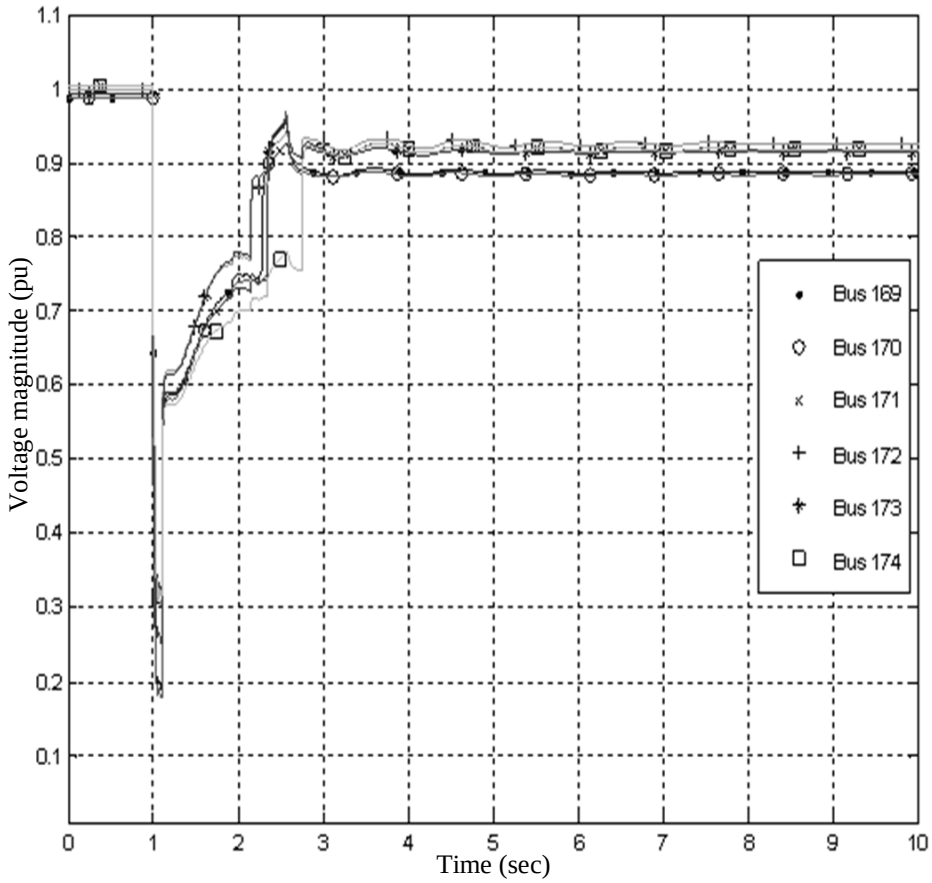

Figure 5.19 Load bus voltage magnitude with final VAr injection values (fault at bus 128) set-2

Figures 5.16 - 5.19 show that the load buses voltage recovery for the different contingencies is very similar to the one of the base case. Actually, it is even better for some contingencies, since the base contingency is the most severe. Therefore, the final set of VAr injection values which was evaluated using the optimization process is also valid for different contingencies, as well as different operating conditions.

CHAPTER 6

CONCLUSIONS AND FUTURE RESEARCH

6.1 Conclusions

This work examines the voltage instability issue in a power system in the presence of significant induction motor loads and applies dynamic VAr injection as a counter-measure to ensure voltage stability following a large disturbance. The system under study has significant amounts of motor load which causes the voltage response at low voltage buses to be highly nonlinear and discontinuous due to the dynamic behavior of motors. Therefore, short term voltage instability, in the form of voltage recovery delay and fast voltage collapse, is considered as the main threat to overall system stability in this work. Short term voltage instability issue is exacerbated by single phase low inertia motor loads which represent residential A/C systems, since they tend to decelerate and stall when their voltage magnitude drops below a certain level. Motors have an adverse impact on voltage stability because they consume very large amounts of reactive power within a very short time during a large disturbance. Therefore, using fast dynamic VAr injection devices was found to be useful in alleviating reactive power deficiency near load centers throughout this work.

Time domain dynamic analysis was used to evaluate the trajectory voltage sensitivities which proved their capability of describing voltage response with respect to injected reactive power. Using trajectory voltage sensitivities as weighting factors in the optimization process resulted in assigning an optimum amount of reactive power injection for each high voltage bus under study, and therefore,

determining the optimal SVC size for each bus. The optimization process was also useful in determining the optimal locations for SVCs since some buses were either not assigned any VAr injection at all, or assigned very small (negligible) amounts. This work also shows that the optimal amount of VAr injection assigned for each bus is inversely proportional to the bus voltage sensitivity. This result is related to the nature of SVC controls operation, and it leads to injecting more VArs into the system during a large disturbance. Different operating conditions where the system is more stressed and different contingencies were also inspected throughout this work to ensure the optimization process robustness and completeness. The final values for SVCs optimal sizes were chosen from different operating conditions in order to form a worst case scenario set. This final set has improved short term voltage stability when tested on a range of operating conditions and contingencies.

6.2 Future work

This work considers SVCs as the main dynamic VAr injection device, and therefore performs the optimization process for determining the required rating of SVCs. However, since the reactive power output of SVCs is proportional to the voltage magnitude squared, which is considered a major drawback for SVCs, other dynamic VAr injection devices such as STATCOMs should be evaluated. Since the VAr output of STATCOMs is linearly proportional to the voltage magnitude, it is expected that less VArs would be needed if SVCs were replaced with STATCOMs.

A range of operating conditions and contingencies were used throughout this work to evaluate and validate the final optimal VAr injection set. However, topological changes should also be considered and their effect on voltage sensitivities should be examined since voltage sensitivities play a major role in the optimization process.

Time domain dynamic analysis is the main tool used in this work to evaluate trajectory voltage sensitivities. Therefore, more improved and comprehensive dynamic models should be developed especially for dynamic loads, since the accuracy of dynamic analysis depends largely on the accuracy of the dynamic models used.

This work used time domain dynamic simulations and linear optimization to evaluate the trajectory voltage sensitivities and optimal VAr injection requirements quantitatively for a specific power system. The same problem should be approached analytically using more comprehensive optimization methods such as Mixed Integer Dynamic Optimization (MIDO), where trajectory voltage sensitivities would be used among many other constraints. The results of such approaches should be compared to the results of this study.

REFERENCES

[1] B. Lesieutre, D. Kosterev, J. Undrill, “Phasor modeling approach for single phase ac motors,” *IEEE Power Engineering Society General Meeting*, 2008, pp. 1-7.

[2] P. Kundur, “Power system stability and control,” McGraw Hill, New York, 1994.

[3] S. Meliopoulos, V. Vittal, J. McCalley, V. Ajjarapu, and I. Hiskens, "Optimal allocation of static and dynamic VAr resources,” *PSERC Publication*, March 2008.

[4] V.S. Kolluri, and S. Mandal, "Determining reactive power requirements in the southern part of the entergy system for improving voltage security – A case study,” *IEEE Power System Conference and Exposition*, 2006, pp. 119-123.

[5] P. Pourbeik, R. Koessler, W. Quaintance, and W. Wong, "Performing comprehensive voltage stability studies for the determination of optimal location, size and type of reactive compensation,” *IEEE Power System Conference and Exposition*, 2006, pp. 118.

[6] IEEE Task Force on Load Representation for Dynamic Performance, “Load representation for dynamic performance analysis,” *IEEE Trans. Power Systems*, 1993, vol. 8, no.2, pp. 472-482.

[7] IEEE Task Force for Load Representation for Dynamic Performance, “Standard models for power flow and dynamic performance simulation*,” IEEE Trans. Power Systems*, 1995, vol. 10, no. 3, pp. 1302-1313.

[8] K. Morison, H. Hamdani, and L. Wang, “Practical issues in load modeling for voltage stability studies,” *IEEE Power Engineering Society General Meeting*, 2003, vol. 3, pp. 1392-1397.

[9] D. Kosterev, A. Meklin, J. Undrill, B. Lesieutre, W. Price, D. Chassin, R. Bravo, and S. Yang, “Load modeling in power system studies: WECC progress update,” *IEEE Power Engineering Society General Meeting*, 2008, pp. 1-9.

[10] G. K. Stefopoulos and A. P. Meliopoulos, “Induction motor load dynamics: Im-pact on voltage recovery phenomena,” *IEEE Power Engineering Society Transmission and Distribution Conference and Exhibition*, 2006, pp. 752-759.

[11] L. Taylor, R. Jones, and S. Halpin, “Development of load models for fault induced delayed voltage recovery dynamic studies,” *IEEE Power and Energy Society General Meeting*, 2008, pp. 1-7.

[12] X. Zheng, R. He, and J. Ma, “A new load model suitable for transient stability analysis with large voltage disturbances,” *Electrical Machines and Systems (ICEMS)*, 2010, pp. 1898 – 1902.

[13] K. Rudion, H. Guo, H. Abildgaard, Z. A. Styczynski, "Non-linear load modeling - requirements and preparation for measurement,” *IEEE Power & Energy Society General Meeting*, 2009, pp. 1-7.

[14] V. Stewart and E. H. Camm, “Modeling of stalled motor loads for power system short term voltage stability analysis,” *IEEE Power Engineering Society General Meeting*, 2008, vol. 2, pp. 1887-1892.

[15] P. Pourbeik and B. Agrawal, “A hybrid model for representing air-conditioner compressor motor behavior in power system studies,” *IEEE Power Engineering Society General Meeting*, 2008, pp. 1-8.

[16] B. Sapkota, and V. Vittal, "Dynamic VAr planning in a large power system using trajectory sensitivities,” *IEEE Transactions on Power Systems*, 2010, pp. 461 – 469.

[17] P. Pourbeik, D. Wang, and K. Hoang, “Load modeling in voltage stability studies,” *Power Engineering Society General Meeting*, 2005, pp. 1893 – 1900.

[18] C. Taylor, “Power system voltage stability,” MC Graw Hill, New York, 1994.

[19] T. Yong, M. Shiying and Z. Wuzhi, “Mechanism research of short-term large-disturbance voltage stability,” *International Conference on Power System Technology*, 2006, pp. 1-5.

[20] P. Li, B. Zhang, C. Wang, J. Shu, M. You, Y. Wang, Z. Bo, A. Klimek, “Time-domain simulation investigates short-term voltage stability with dynamic loads,” *Asia-Pacific Power and Energy Engineering Conference*, 2009, pp. 1-5.

[21] J. Diaz de Leon II, and C. Taylor, “Understanding and solving short-term voltage stability problems,” *IEEE Power Engineering Society Summer Meeting*, 2002, vol. 2, pp. 745 – 752.

[22] C. Sharma, and M. Ganness, "Determination of power system voltage stability using modal analysis,” *International Conference on Power Engineering, Energy and Electrical Drives*, 2007, pp. 381 – 387.

[23] M.Hasani and M.Parniani, "Method of combined static and dynamic analysis of voltage collapse in voltage stability assessment,” *IEEE Transmission and Distribution Conference and Exhibition: Asia and Pacific*, 2005, pp. 1-6.

[24] T. Cutsem, and C. Vournas, “Voltage stability of electric power systems,” Kluwer Academic Publishers, 1998.

[25] V. Vittal, “Transient stability test systems for direct stability methods,” *IEEE Transactions on Power Systems*, 1992, pp. 37-43.

[26] N. Lu, and A. Qiao, “Composite load model evaluation,” Pacific Northwest National Laboratory, September 2007